Environmental Earth Sciences (2021) 80:488
https://doi.org/10.1007/s12665-021-09775-4

ORIGINAL ARTICLE

Nb–Sr–Pb isotope analysis in soils of abandoned mercury quarry in northwest Black Sea (Turkey), soil and plant geochemistry, evaluation of ecological risk and its ımpact on human health

Bilgehan Yabgu Horasan[1] · Alican Ozturk[2] · Osman Tugay[3]

Received: 27 February 2021 / Accepted: 9 July 2021

Abstract

Potential toxic element accumulation in soils and plants is one of the leading environmental problems in recent years. In many countries, mining enterprises are generally abandoned for reasons such as increasing costs, depleted reserves, and changes in ore quality. The negative effects on the environment during or as a result of these activities are known. The focus is on investigating the Hg concentration accumulated in the soil and plants around the abandoned mercury quarry located in the north-west Black Sea region (Tezcan Hg Mine). While the distribution of Hg and As is observed toward the downward slope in the mining area, it has been observed that it decreases as it moves away from the source area. The relationship of Hg concentration with granite intrusions in the areas of upward slope and topographic barriers is due to the alteration of the hydrothermal phase mineralizations and the accumulation of ore rocks. According to the Geoaccumulation Index in the lands around the abandoned mercury quarry in the Northwest Black Sea region, AsI_{geo} and HgI_{geo} accumulation are found as extremely; according to contamination factor, CF_{As} and CF_{Hg} values are found as very high; according to enrichment factor, EF_{As} and EF_{Hg} are found as extremely high; according to the Potential Ecological Risk Factor, As and Hg are found as very risky, and according to the Pollution Load Index, they are found as Pollution. As well as in soils, As and Hg concentrations were determined in *Mentha longifolia* (L.) L. subsp. *typhoides* (Briq.) Harley (dere nanesi) from the Lamiaceae (Turkish name: Ballıbabagiller) family, *Taraxacum buttleri Van* Soest (karahindiba) from the Asteraceae (Turkish name: Papatyagiller) family, *Plantago lanceolata* L. (damarlıca) from Plantaginaceae (Turkish name: Sinirotugiller) family, and *Pyracantha coccinea* M. Roem. (ateşdikeni) from the Rosaceae (Turkish name: Gülgiller) family, which were collected from the same locations. According to $^{207}Pb/^{206}Pb$—$^{208}Pb/^{206}Pb$, the origin of lead in the soils within the enterprise is of geogenic origin, and according to the results of $^{87}Sr/^{86}Sr$—$^{143}Nd/^{144}Nd$, it is thought that the samples examined are caused by granitoid.

Keywords Kastamonu · Mercury · Ecological risk · Pb–Sr–Nd isotopes · Soil geochemistry · Plant geochemistry

Introduction

Mining enterprises are generally closed due to increasing costs, depleted reserves, changes in ore quality, environmental impacts, and geological factors. Mining activities can harm the environment even after years (Lottermoser 2007) and are considered to be one of the major sources of environmental pollution worldwide (Rieuwerts et al. 2009; Beane et al. 2016). Active mine tailings from these abandoned mining operations can be a constant source of heavy-metal contamination with toxic effects on living biota, water, and soil (Mileusnic et al. 2014). Although mining operations have a direct positive economic impact, as a result of these activities, a large area of the earth's surface has been contaminated with abundant and uncontrollable heavy-metal

✉ Bilgehan Yabgu Horasan
bilgehanyabgu@gmail.com

Alican Ozturk
alicanozturktr@gmail.com

Osman Tugay
otugay@selcuk.edu.tr

[1] Department of Environmental Protection and Technologies, Selcuk University Sarayonu Vocational School of Higher Education, Sarayönü, Konya, Turkey

[2] Department of Geological Engineering, Faculty of Engineering and Natural Sciences, Konya Technical University, Selçuklu, Konya, Turkey

[3] Department of Pharmaceutical Botany, Faculty of Pharmacy, Selcuk University, Selçuklu, Konya, Turkey

Published online: 22 July 2021

releases (Sebei et al. 2020). Potential toxic elements (PTE) can come from the soil, streams, sediments, and anthropogenic or geological sources. Besides, PTEs pose a significant environmental and public health risk worldwide by contamination and degradation of environmental matrices (Yi et al. 2011; Yalcin et al. 2019; Horasan and Arik 2019). The adverse effects caused by direct exposure of people to PTEs are through skin contact and ingestion of contaminated particles, inhalation, and indirect exposure to PTEs taken through the food chain (Xiao et al. 2017). Toxic elements that develop due to mine site wastes (Such as Coal, Hg, Cu etc.) affect fauna with direct adverse effects on soil microbial activity and diversity (Altay and Dumlupinar 2013;Alvarez et al. 2017; Li et al. 2017; Chen et al. 2018).

Elements that accumulate in the soil are transferred to the plant by plant roots and are included in the food chain through living things that feed on these plants (Kabata-Pendias 2004; Durguti et al. 2020). For this reason, estimating the dimensions of the pollution caused by PTEs in the vicinity of the mining sites is the first condition to be done before action be taken in these areas. Toxic elements, which are also found in mining wastes, spread to the environment from the area where the wastes are stored. This distribution can occur as a result of natural events such as erosion (water and wind), human factors, landslides, flooding, and geological events. Mining activities are one of the most polluting activities in the world, and it is also known to cause the loss of biodiversity developing around it (Mammola et al. 2019). The study area is located in Kastamonu, Turkey, north-west (Bozkurt) remains in the province. Mercury mining was carried out intermittently in the region between 1960 and 1990 and was later abandoned. Besides, the ore extracted from the quarry was melted near the operation and the waste generated was stored irregularly in the mine site. Mercury is among the dangerous pollutants that threaten aquatic ecosystems and human health in many parts of the world. It has a large bioaccumulative and biological capacity in aquatic and terrestrial ecosystems (Horvat 2002).

In the research area, there was no study about the abandoned mine in the previous years, and with this study, the effects of the wastes of the abandoned mercury on the soil and plants were investigated, and distribution maps and ecological risk factors were determined. First of all, the geological characteristics of the region were examined and the regions that could be geogenic and anthropogenic resources were determined and examined. In addition to the ecological risk assessment of the mine site and surrounding soils, studies were carried out to determine the genesis by performing Sr–Nb–Pb isotope analyses. The quarry and its surroundings have been found as high-risk polluted areas according to ecological risk indices. The area where the research was conducted remains in the Black Sea climate (rainy and humid in all seasons) in the north-west region of Turkey. Mercury and arsenic elements have been dispersed and accumulated due to the sloping morphology in the region with the effect of pollution and precipitation. Thus, the distribution of Hg and As was exhibited in the slope lower regions. However, the accumulation in the region does not only develop due to the furnace and melting factors; morphologically, the presence of Hg values above the pollution source indicates that it accumulates geogenically. In the study, natural morphological barriers and climatic properties controlled the Hg distribution. The concentration of plants was dependent on the Hg concentration in the soil, and the results of plant analysis were high in the regions where it was high, and low results were obtained in the regions where low Hg concentrations were observed in the soil.

Materials and methods

This study was carried out to determine the accumulations on the abandoned mercury deposit and the surrounding soil and plants, to determine the risks, and to determine the distribution. For this purpose, three basic parts are designed for us to work. Geology, soil, and plant types were studied. For the first stage (examining the region and collecting samples), 21 soil and 11 plant samples that would represent the region best were collected (Fig. 1). Soil groups were collected from the vicinity of the gallery, the areas where melting and separation took place, and the surrounding of the waste site. The following plants have been considered as study material, because they are common plants in the study area and they are used in different ways by local people. A total of 11 samples (belong to four different taxa) were taken from *Mentha longifolia* subsp. *typhoides* (dere nanesi) from the Lamiaceae (Turkish name: Ballıbabagiller) family, *Taraxacum buttleri* (karahindiba) from the Asteraceae (Turkish name: Papatyagiller) family, *Plantago lanceolata* (damarlıca) from Plantaginaceae (Turkish name: Sinirotugiller) family, and *Pyracantha coccinea* (ateşdikeni) (Turkish name: Gülgiller) from the Rosaceae family (Davis 1972, 1975, 1982; Güner et al. 2012), which are widely observed in the study area. For the second stage (Preparation for analysis), plant samples from the study area, along with the root stem and flower parts, were taken and put into a double bag. Soil samples, on the other hand, by considering the geology (fault, lithology etc.), morphology, weathering, abrasion, and transporting factors of the region and the areas where the mining and operation processes take place were taken from the bedrock, close to the mine and operation areas from a depth of about 20 cm and placed in a double bag and brought to the laboratory and then dried in a special oven at 40 °C for 24 h. Later, the samples crushed with a plastic mallet were ground and reduced to 80 mesh, 200 g of sample was taken, and the remaining part was kept as a witness sample

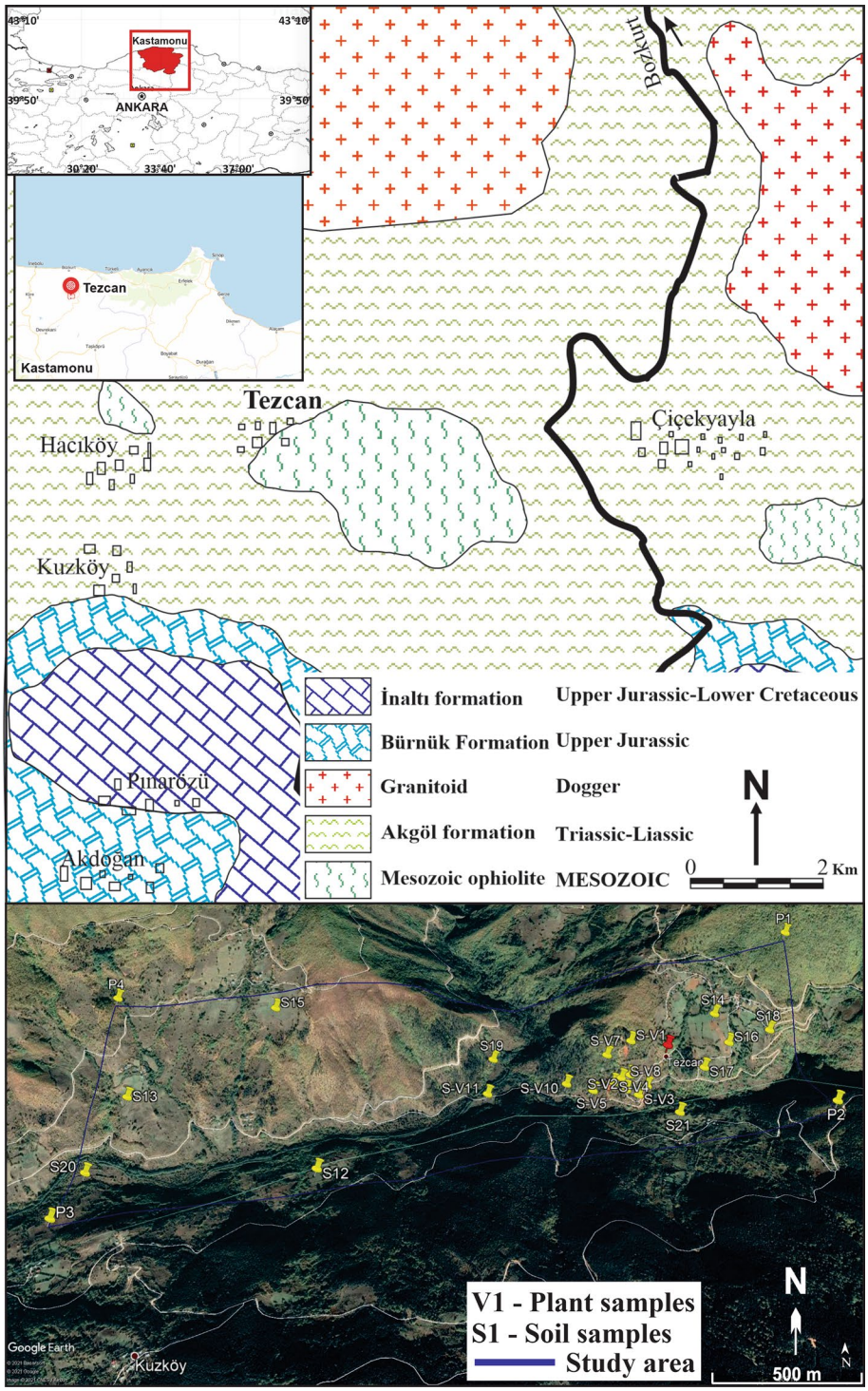

Fig. 1 Study area boundaries and geology map (edited from Uguz and Sevin 2007)

for further analysis. The impurities in the plants were first cleaned with a brush, then washed with a dilute hydrochloric acid solution (5%), acetic acid solution (2%), and detergent solution (0.1%), and then rinsed with distilled water. Since the presence of water in the plant caused the continuation of the metabolic activity, the samples were dried rapidly. Soil and plant samples prepared were analyzed following Acme Analytical Laboratories Limidet (Vancouver-Canada). AQ250 analysis package, which is the standard package of Acme Analytical Laboratories, was chosen for soil analysis. This package includes Mo, Cu, Pb, Zn, Ag, Ni, Co, Mn, Fe, As, U, Au, Th, Sr, Cd, Sb, Bi, V, Ca, PLa, Cr, Mg, Ba, and Ti, and it includes the elements B, Al, Na, K, W, Sc, Tl, S, Hg, Se, Te, and Ga. For these analyses, first, the sample was

reduced to 5 mm in a milling machine, 0.5 g for soils, 1 g for plants, samples were taken from the sample, which was thinned down to 75 µ, in accordance with the laboratory procedure for analysis. The prepared sample is digested with a modified Aqua Regia solution of equal parts concentrated HCl, HNO_3, and DI H_2O for one hour in a heating block or hot water bath. The sample is made up to volume with dilute HCl. VG100 analysis package, which is the standard package of Acme Analytical Laboratories, was selected for plant analysis. This package includes Mo, Cu, Pb, Zn, Ag, Ni, Co, Mn, Fe, As, U, Au, Th, Sr, Cd, Sb, Bi, V, Ca, P, La, Cr, Mg, Ba Ti, B, Al, Na, K, W, Sc, Tl, S, Hg, Se, Te, and Ga elements. The prepared sample is cold leached with nitric acid and then digested in a hot water bath. After cooling a modified Aqua Regia solution of equal parts, concentrated HCl, HNO_3, and DI H_2O are added to each sample to leach in a heating block of hot water bath. STD DS11 and STD OREAS262 were used for soil analysis, and STD CDV-1 and STD V16 were used in plant analysis. This reference material contains the elements in the analysis package and is calculated with an error of 10% ± from the expected value. In case it is out of the standard deviation, the analyses were carried out in accordance with Quality Assurance/Quality Control (QA/QC). For the third stage (data evaluation), cluster analysis, basic statistical parameters, and main component analysis were made on the acquired info. Besides, the pollution potential and degree of the region in terms of Igeo, EF, C_f, Er, and RI factors of Hg, Pb, Cr, Zn, Cu, As, Mn, Al, Cd, and Fe elements were calculated. In addition, distribution maps of the study area were prepared.

Lead (Pb), Strontium (Sr), and Neodymium (Nd) isotope geochemistry experiments were carried out in the Central Laboratory of the Middle East Technical University. The process monitored by the laboratory has been conveyed. Weighing, chemical solving, and chromatography processes were carried out using ultra-pure water and chemicals at 100 cleanliness standards under clean laboratory conditions. Approximately 100 mg of the samples were weighed and transferred to PFA bottles. The samples were completely thawed by keeping them in 4 mL of 52% HF for 4 days on a heating plate of > 100 tabC, and then, they were again dried on the heater and placed in 1 mL 2.5 N HCl and made ready for chromatography. Strontium was separated in Teflon columns using a 2 mL volume of Bio-Rad AG50 W-X8 100–200 mesh resin with 2.5 N HCl acid. After strontium collection, the rare soil fraction was collected with 6 N HCl. Strontium was loaded onto the single Re-filament using Ta-activator and 0.005 N H3PO4 and measured in static mode. $^{87}Sr/^{86}Sr$ data are normalized to $^{87}Sr/^{86}Sr = 0.1194$. During the measurements, Sr NBS 987 standard was measured as 0.710257 ± 3. Neodymium element was separated by passing through 2 ml volume of HDEHP (bis-ethyexyl phosphate)-coated biobeads Bio-Rad resin in Teflon columns using 0.22 B HCl acid from other rare-earth elements. Separated neodymium was loaded into the Re-filament together with 0.005 N H_3PO_4 and measured in static mode using the double-filament technique. During the analyses, the data $^{143}Nd/^{144}Nd$ were normalized to $^{143}Nd/^{144}Nd = 0.7219$. The standard of Nd Lajolla was measured as 0.511837 ± 3 ($n = 2$). No bias correction was made on the results of Sr and Nd isotope ratio measurement. In accordance with the quality assurance system, the quality level of the entire process is periodically checked with the USGS rock standards, which are measured under the same conditions by passing through the same chemical processes with the samples in METU central laboratories. For lead isotope ratio analysis, 80 mg of each sample was weighed and dissolved on the heater using HF and 6 N HCl acids, respectively, and the samples were prepared for chromatography by adding 1 mL of 2 N HCl. The lead element was separated using Bio-Rad AG1-X8 anion exchange resin and HCl and HBr acids in Teflon columns and loaded by adding silica gel and 0.005 N H_3PO_4 to the single filament. Measurements were made in static mode in the temperature range of 1150–1250 °C. The NIST SRM981 standard gave 16.940, 15.490, and 36.888 ($n = 6$) values for $^{206}Pb/^{204}Pb$, $^{207}Pb/^{204}Pb$, and $^{208}Pb/^{204}Pb$ ratios, respectively, and the required bias correction was made on the results by considering the NBS reference values. Isotope ratio measurements were made by multiple summations using the Triton Thermal Ionization Mass spectrometer (Thermo-Fisher). Analytical uncertainties are at the level of 2 sigmas.

Geological settings

In the study area, ophiolites and the Triassic-Liassic epi-ophiolitic cover (Akgol formation) of these ophiolites were thrust over the Bekirli formation, which is considered to be the metamorphic counterpart of this cover. Continental crustal metamorphic rocks (Devrekani metamorphics) are also thrust on this oceanic crust material. Combined with tectonic effects that were damped in early Dogger, these ancient rocks are cut by Dogger aged granitoid and transgressively overlain by a sedimentary sequence starting with Malm and lasting until the Lutetian (Fig. 1) (Uguz and Sevin 2007).

Pollution assessment methods

In this study, Contamination factor (CF), Enrichment factor (EF), Ecological risk ındex (RI), Geoaccumulation ındex (Igeo), Pollution load index (PLI), and Potential Ecological risk factor (E_r^i) were calculated according to the formulas in (Table 1). The results obtained are evaluated according to Table 2.

Table 1 Selected soil pollution indices

Common designation	Expression	References
Geoaccumulation index (I_{geo})	$I_{geo} = \log_2 C_n/1.5\ B_n$ C_n: the measured concentration of the examined metal i in the sediment, B_n: the geochemical background concentration or reference value of the metal Factor 1.5 is used because of possible variations in background values for a given metal in the environment	(Muller 1969)
Contamination factor (C_f)	$C_f = C_{metal}/C_o$ C_{metal}: metal concentration of the sample C_o: background value of metal	(Hakanson 1980)
Pollution loading index(PLI)	$PLI = n\sqrt{(C_{F1} * C_{F2} * C_{F3} * \ldots * C_{Fn})}$ C_f: pollution factor n: metal number	(Tomlinson et al. 1980)
Enrichment factor (EF)	$EF = (C_x/Fe_x)/(C_c/Fe_c)$ C_x, Fe_x: measured heavy metal concentration C_c, Fe_c: the basic (background) value of metal (for Fe)	(Zoller et al. 1974)
Potential ecological risk index (E_r^i)	$E_r^i = T_r^i \times C_f$ T_r^i: the toxic-response factor for a given substance C_f: contamination factor	(Hakanson 1980)
Potential toxicity index (RI)	$RI = \sum_{i=1}^{n} E_r^i$ E_r^i: the single index of ecological risk factor	(Hakanson 1980)

Table 2 Soil contamination classification (Muller 1969; Hakanson 1980; Tomlinson et al. 1980; Zoller et al. 1974)

Soil pollution index	Potential ecological risk						
Igeo	Igeo < 0 unpolluted	0 < Igeo < 1 unpolluted to moderately	1 < Igeo < 2 moderately	2 < Igeo < 3 moderately to strongly	3 < Igeo < 4 strongly	4 < Igeo < 5 strongly to extremely	Igeo > 5 extremely
C_f	$C_f < 1$ low	$1 < C_f < 3$ moderate	$3 < C_f < 6$ considerable	$C_f > 6$ very high			
PLI	PLI > 1 pollution	PLI < 1 unpollution					
EF	EF < 2 depletion to mineral	2 < EF < 5 moderate	5 < EF < 20 significant	20 < EF < 40 very high	EF > 40 extremely high		
E_r^i	$E_r^i < 40$ low	$40 \le E_r^i < 80$ moderate	$80 \le E_r^i < 160$ considerable	$160 \le E_r^i < 320$ high	$E_r^i \ge 320$ very		
RI	RI < 150 low	150 ≤ RI < 300 moderate	300 ≤ RI < 600 considerable	RI ≥ 320 very high			

Results

Soil geochemistry

The study area is located in the north of Turkey due to its location, and there is a spread of podzolic soils (typical of cold and humid regions) in this section, whose altitude increases as you go inland from the coast (Dengiz et al. 2016). On soil samples taken for this study, concentration values of Mo, Cu, Pb, Zn, Ag, Ni, Co, Mn, Fe, As, U, Au, Th, Sr, Cd, Sb, V, Ca, P, La, Cr, and Mg were determined. Ecological pollution index evaluation of Cu, Pb, Zn, Ni, Mn, Fe, As, Cd, Cr, Al, and Hg trace elements was made. (Table 3). Ecological pollution index evaluation of Zn, Cu, Fe, Pb, Ni, Mn, As, Al, Cr, Hg, and Cd trace elements were made. Furthermore, these elements are evaluated according to Turkey's soil pollution limit values and the values of some countries (Table 4). According to soil pollution values in Turkey, the average values of Mercury and arsenic are above the limit values, as well as the values of soil pollution in some countries

Table 3 Soil analysis result (ppm)

	Mo	Cu	Pb	Zn	Ag	Ni	Co	Mn	Fe	As	U	Au	Th	Sr	Cd	Sb	V	Ca	P	La	Cr	Mg	Ba	Ti	Al	Na	K	W	S	Hg
S_{TEZ}-1	0.9	22	29	102	0.066	85	22	847	49,400	4424	0.8	0.0012	2	52	0.5	369	22	83,700	600	6	20	36,200	106	10	8000	10	1800	3	500	500
S_{TEZ}-2	0.8	20	30	100	0.065	78	21	819	48,700	4404	0.7	0.0018	2	52	0.4	338	22	92,900	560	5	21	40,500	90	10	7800	10	1700	2	600	500
S_{TEZ}-3	0.8	21	30	94	0.07	83	20	815	47,600	4326	0.8	0.0033	2	52	0.5	350	22	90,000	560	6	20	39,000	93	10	7700	10	1800	2	500	500
S_{TEZ}-4	0.86	24	51	132	0.135	137	41	1442	67,400	10,000	2.2	0.0357	4	96	0.7	1301	39	81,400	780	13	36	41,300	167	90	22,300	290	5200	6	8400	441
S_{TEZ}-5	0.86	24	52	135	0.144	140	38	1404	67,100	10,000	2.2	0.0376	5	102	0.7	1239	42	87,200	770	14	36	44,400	161	120	22,900	300	5400	7	9100	500
S_{TEZ}-6	0.86	19	31	98	0.078	80	21	909	49,000	4342	0.8	0.0153	2	54	0.4	430	23	88,900	590	6	22	39,700	105	10	8300	10	1900	3	800	500
S_{TEZ}-7	0.78	20	32	99	0.067	77	20	786	50,200	4343	0.8	0.0025	2	51	0.4	425	21	86,300	550	6	21	37,800	90	10	7700	10	1700	3	500	500
S_{TEZ}-8	1.15	33	52	177	0.136	129	35	892	99,000	10,000	2.2	0.0332	4	101	0.9	1384	39	38,300	920	16	50	16,100	204	40	18,900	270	4300	4	500	500
S_{TEZ}-9	1.26	34	58	180	0.143	126	36	879	97,900	10,000	2.3	0.0342	5	104	0.8	1320	39	36,400	910	16	53	15,200	204	30	19,300	260	4400	4	500	500
S_{TEZ}-10	0.83	21	51	158	0.127	133	34	1643	77,600	10,000	2.4	0.0346	5	106	0.8	1134	46	85,000	610	15	42	45,600	211	120	25,700	180	4300	5	3400	376
S_{TEZ}-11	0.72	45	23	100	0.055	83	19	761	39,400	30	0.3	0.0026	3	24	0.1	0.4	31	13,500	510	6	63	7700	109	20	16,000	290	3000	0.1	300	21
S_{TEZ}-12	0.74	43	24	91	0.06	82	17	768	39,100	30	0.3	0.0023	3	16	0.1	0.7	33	4300	600	8	68	7600	122	20	17,900	360	3800	0.1	500	2
S_{TEZ}-13	0.68	40	19	81	0.045	78	15	564	22,500	25	0.1	0.0012	2	14	0.1	0.3	28	11,000	500	5	45	6800	90	10	14,500	320	2000	0.1	100	1
S_{TEZ}-14	0.69	39	18	86	0.036	99	16	665	37,500	17	0.2	0.0015	2	14	0.1	0.4	27	8700	600	5	40	7800	81	20	12,300	250	3000	0.1	300	5
S_{TEZ}-15	0.79	46	15	95	0.054	79	11	489	36,800	35	0.3	0.0021	3	14	0.1	0.5	24	5600	450	6	35	5500	110	10	9800	150	2500	0.1	400	1
S_{TEZ}-16	0.55	23	19	82	0.055	98	16	789	29,600	19	0.1	0.00201	3	12	0.1	0.5	31	8900	400	5	22	4500	100	10	7800	10	1400	0.1	500	3
S_{TEZ}-17	0.59	56	24	70	0.041	88	13	412	25,800	30	0.4	0.0011	3	17	0.1	0.7	27	9700	500	8	37	6800	101	10	6800	10	3500	0.1	600	9
S_{TEZ}-18	0.64	41	18	99	0.021	65	15	658	35,400	45	0.2	0.0018	3	11	0.1	0.8	15	4700	650	7	56	4800	102	10	9500	10	2900	0.1	100	4
S_{TEZ}-19	0.48	42	16	87	0.035	54	13	702	36,500	35	0.2	0.0014	3	16	0.1	0.1	18	2300	300	6	55	7800	91	20	11,500	320	4000	0.1	100	22
S_{TEZ}-20	0.39	25	14	78	0.064	75	12	687	29,700	28	0.1	0.0019	2	10	0.1	0.3	21	6800	500	6	49	8800	89	10	12,300	150	4500	0.1	200	17
S_{TEZ}-21	0.41	45	18	84	0.018	69	13	524	30,600	24	0.3	0.0017	2	15	0.1	0.4	22	9800	550	7	41	7500	105	20	14,800	10	2500	0.1	300	1
Min	0.39	19	14	70	0.018	54	11	412	22,500	17	0.1	0.0011	2	10	0.1	0.1	15	2300	300	5	20	4500	81	10	6800	10	1400	0.1	100	1
Max	1.26	56	58	180	0.144	140	41	1643	99,000	10,000	2.4	0.0376	5	106	0.9	1384	46	92,900	920	16	68	45,600	211	120	25,700	360	5400	7	9100	500
S. Dev	0.2	12	15	34	0.04	27	10	347	23,513	4180	0.9	0.015	1	37	0.3	542	9	38,137	168	4	16	16,526	44	38	6150	138	1309	2	2878	239

Table 4 The comparison of maximum limit values given for certain elements in the soils of Turkey (MOEF 2001) and other countries (Kabata-Pendias and Pendias 2004) with the values obtained (ppm)

Country	Austria	Poland		Germany		E.U	Russia	England	USA		Turkey	This study		
Element	1977	1977	1993	1984	1992	1986	1986	1987	1988	1993	2001	Mean	Min	Max
As	50	–	30	20	–	–	2	10	14	–	20	3436	17	10,000
Cd	5	1	3	3	1,5	1–3	–	3–15	1,6	20	1	0,34	0,08	0,88
Co	50	–	50	–			–	–	20		20	21	11	41
Cr	100	80	50	100	100	50–150	0,05	–	120	1500	100	40	20	68
Cu	100	70	30	100	60	50–140	23	50	100	750	50	32	19	56
Mo	10	–	10	–	–	–	–	–	4	–	10	0,75	0,39	1,26
Ni	100	75	30	50	50	30–75	35	20	32	210	30	92	54	140
Pb	100	150	70	100	100	50–300	20	500–2000	60	150	50	30	15	58
Zn	300	300	100	300	200	150–300	110	130	220	1400	150	106	70	170
Ba											200	121	81	211
Hg											1	400	1	1000

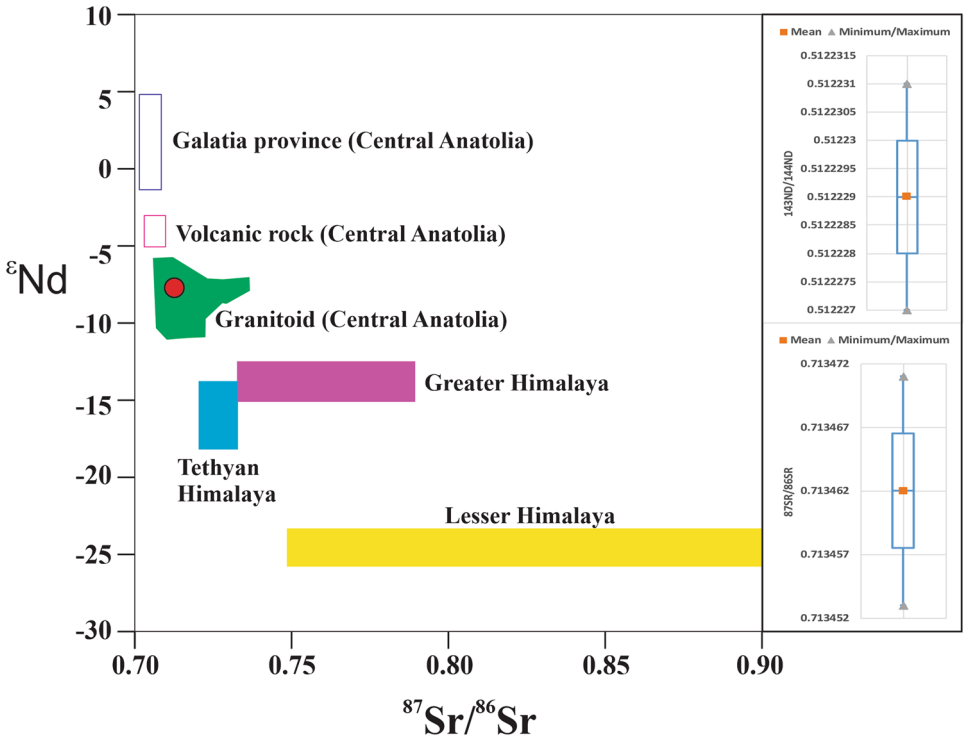

Fig. 2 Diagram of $^{87}Sr/^{86}Sr$ with Figure $^{\varepsilon}Nd$ (Galatia region-Central Anatolia, Wilson et al. 1997; Central Anatolia volcanic rocks, Alpaslan et al. 2004; Central Anatolian granitoids, Köksal and Göncüoğlu 2007; Great Himalaya, Tethyan Himalayan and Small Himalaya, Bracciali et al. 2015; Eker et al. 2018) and error bars on the isotope plots

around the World (Table 4). It was found that Hg and As values in the direction of the slope were above the limit values depending on the topographic slope, and Mercury and arsenic values in the upper codes from the location were low in soil concentrations (Fig. 2). Other fractions (Cu, Co, PB, Ni, and Cd) are below the Turkish soil pollution limit.

Bioaccumulation

In this study, 11 plant samples were collected from the mine, smelting facility, and its wastes. Concentrations of Mo, Cu, Pb, Zn, Ag, Ni, Co, Mn, Fe, As, U, Au, Th, Sr, Cd, Sb, V, Ca, P, La, Cr, Mg, Ba, Ti, Al Na, K, W, S, and Hg in plants were determined (Table 5). The study area in the Western Black

Sea region is in a forest area covered with dense trees. In the study area, larch, scotch pine, oak and fir, and fern undercover occupy an important place (Dengiz et al. 2016). In this study, samples were taken from *Mentha longifolia* subsp. *typhoides* (dere nanesi) from the Lamiaceae (Turkish name: Ballıbabagiller) family, *Taraxacum buttleri* (karahindiba) from the Asteraceae (Turkish name: Papatyagiller) family, *Plantago lanceolata* (damarlıca) from Plantaginaceae (Turkish name: Sinirotugiller) family, and *Pyracantha coccinea* (ateşdikeni) from the Rosaceae (Turkish name: Gülgiller) family (Davis 1972, 1975, 1982; Güner et al. 2012). *Mentha longifolia*, taken from locations 1 and 5, is also known as feathered mint, long-leaved mint, wild mint, and punk. This plant is a perennial plant and prefers sunny or semi-shady areas in moist soil. It is variable; it can be hairy, moldy, or have a pungent odor. Flowering stems vary between 40 and 120 cm. Its leaves and flowering branches have a mint-based aroma and are consumed because of their antispasmodic, carminative, and stimulating effects (Davis 1982). Looking at the amount of PTE in the soil at the location of the plant samples taken, noteworthy arsenic and mercury concentrations are exceeding the limit values of PTE in the territory of Turkey. Arsenic concentration value in soil S1, where Mentha longifolia species was taken at locations 1 and 5, is 4423.5 ppm, while the value of the plant is 32.1 ppm, the mercury value in the soil is 500 ppm, and in the plant, it is 1.27 ppm. At location S5, the concentration value of arsenic in the soil is 10,000 ppm, while the concentration in the plant is 206.8 ppm, and while the concentration of mercury in the soil is 500 ppm, it is 1.25 ppm in the plant (Table 5). Taraxacum butts Van Soest plant taken from locations 2, 3, 4, and 8 is a perennial plant that grows in sunny or semi-shaded areas in moist soils. The plant is small with few leaves, short, and the edges of the lobes have three corners; the petiole shows pink features. It generally grows on roadsides, fields, rocky areas, at altitudes between 150 and 2300 m, and is known to be consumed raw by local people (Karatas 2007). The arsenic concentrations in the soil at locations 2, 3, 4, and 8 were 4403.7 ppm, 4325.7 ppm, 10,000 ppm, and 10,000 ppm, respectively; and mercury concentrations are 500 ppm, 500 ppm, 441 ppm, and 500 ppm, respectively. In plants, the arsenic values were found to be 150.5 ppm, 76.9 ppm, 1674.2 ppm, and 1430.9 ppm and the mercury values were found to be 4.25 ppm, 7.93 ppm, 6.87 ppm, and 7.75 ppm, respectively (Table 5). Plantago lanceolata type plant common name is a narrow-leaved edible herb, also known as vascular. They are perennial plants that grow in permeable, moist, or dry soils, with a flower stem length of 10–60 cm and a leaf length of about 25 cm, resistant to frost, used for human and animal feeding (Kara et al. 2015). The arsenic concentrations in the soil of the samples collected from 6, 9, 10, and 11 locations were found as 4342.4 ppm, 10,000 ppm, 10,000 ppm, and 30 ppm and mercury concentrations were

Table 5 Chemical analysis result in plants (ppm)

	Mo	Cu	Pb	Zn	Ag	Ni	Co	Mn	Fe	As	U	Au	Th	Sr	Cd	Sb	V	Ca	P	La	Cr	Mg	Ba	Ti	Al	Na	K	W	S	Hg
V1	3	7	0.4	55	0.01	8	0.3	63	410	32	0.01	0.00	0.10	10	0.55	5	4	4700	2780	0.07	8	6630	3	9	200	50	47,700	0	12,500	1.27
V2	1	12	2	27	0.01	3	0.6	43	1560	151	0.03	0.00	0.20	21	0.03	18	6	6900	2470	0.32	10	7570	26	11	500	120	11,800	0	2500	4.25
V3	7	16	1	69	0.02	2	0.5	71	1330	77	0.02	0.00	0.10	34	0.11	13	2	16,800	4150	0.16	3	3200	14	10	300	50	25,000	3	3600	7.93
V4	1	16	11	66	0.04	27	6.6	246	17,430	1674	0.32	0.01	0.90	38	0.20	255	17	36,500	2070	1.23	27	13,450	63	11	3900	60	9700	3	2000	6.87
V5	1	16	3	55	0.02	9	1.7	120	3510	207	0.09	0.00	0.30	29	0.05	40	6	17,700	2940	0.44	9	4780	30	10	900	70	13,200	1	2200	1.25
V6	1	10	2	49	0.04	6	1.9	102	3840	349	0.12	0.00	0.30	36	0.05	74	3	17,700	2100	0.34	5	4330	80	10	500	50	9000	1	2200	1.85
V7	2	17	6	69	0.02	5	0.9	96	3230	138	0.04	0.00	0.20	28	0.14	22	5	13,400	2220	0.38	6	3620	21	15	800	30	33,500	1	2100	8.85
V8	2	19	8	118	0.05	24	5.4	203	12,970	1431	0.32	0.01	0.80	59	0.20	233	16	21,200	1610	1.98	22	5490	88	20	3200	70	8800	5	1400	7.75
V9	4	13	4	86	0.02	11	2.5	97	8740	947	0.20	0.00	0.50	68	0.11	185	12	14,800	2470	1.37	19	4800	111	14	1600	50	15,700	6	2100	9.00
V10	1	7	1	57	0.01	2	0.6	48	1600	1001	0.01	0.00	0.10	31	0.04	0.1	2	16,100	1210	0.14	3	1810	115	8	200	70	18,100	0	1900	3.00
V11	0.5	7	1	65	0.01	2	0.4	56	1200	10	0.01	0.00	0.10	32	0.08	18	1	17,100	1650	0.13	9	2250	135	5	750	85	19,100	0	1850	2.50
Min	0.5	6.5	0.4	26.9	0.0	1.6	0.3	43.0	410.0	10.0	0.0	0.0	0.1	9.9	0.0	0.1	1.0	4700.0	1210.0	0.1	3.0	1810.0	2.6	5.0	200.0	30.0	8800.0	0.1	1400.0	1.3
Max	7	19	11	118	0	27	7	246	17,430	1674	0	0	1	68	1	255	17	36,500	4150	2	27	13,450	135	20	3900	120	47,700	6	12,500	9
Mean	2	13	4	65	0	9	2	104	5075	547	0	0	0	35	0	78	7	16,627	2334	1	11	5266	62	11	1168	64	19,236	2	3123	5
S. Dev	2	5	3	23	0	9	2	65	5577	606	0	0	0	16	0	97	6	8181	793	1	8	3218	46	4	1252	24	12,071	2	3157	3

found as 500 ppm, 500 ppm, 376 ppm, and 21 ppm, respectively. The arsenic concentrations in the plant are 349.4 ppm, 946.6 ppm, 1001.1, and 10 ppm and mercury concentrations are 1.85 ppm, 9 ppm, 3 ppm, and 2.5 ppm, respectively (Table 5). The Pyracantha coccinea plant species, taken from location 7, is a perennial plant that likes sandy and clay soils in temperate climates. It is a plant that grows at various attitudes in South and Southeast Europe, Italy, the Balkans, the Crimea, the Caucasus, and Turkey. Firethorn, a member of the Rosaceae family, is a plant that can protect its leaves throughout the year. Firethorn, which is green in all seasons just like pine trees, is used frequently in garden decoration art due to its appearance and this feature. Firefist fruits are particularly rich in-carotene and lycopene (Coteli and Karatas 2017). In soil samples taken from the location, the arsenic concentration is 4343.3 ppm, and the mercury concentration is 500 ppm, respectively. 137.5 ppm arsenic and 8.85 ppm mercury concentrations were determined in the plant (Table 5).

Nb–Sr–Pb ısotope analysis

Pb, Sr, and Nd isotope ratios have been expressed as appropriate tools to identify different sources of pollution in sediments, water (underground–aboveground, lake, sea, and rain), and atmospheric/urban dust and soils (Steinmann and Stille 1997; Kong et al. 2018).

Minerals and rocks have different ratios of $^{87}Sr/^{86}Sr$ and $^{143}Nd/^{144}Nd$, depending upon their geological origin and age, and these isotope ratios do not change much in their elemental composition during the transport or sedimentation phase. Stable isotopes of Sr and Nd elements are of great importance in determining the source and transportation processes of materials (Wenbo et al. 2006). Due to the possibility that the Nd element is less mobile than Sr during weathering and transportation, it is expected to preserve its source origin better in sediments. Therefore, both Sr and Nd isotopic states in sediments can generally be interpreted in terms of source origins (Aberg 1995). Pb isotope data are used to determine both anthropogenic (especially leaded gasoline sourced, Chow and Johnstone 1965) and geogenic (ore formation/mining activities, Gulson et al. 2004) sources of origin (Cuvier et al. 2016).

In isotopic studies carried in the study area, $^{206}Pb/^{204}Pb$ (18.516367 ± 0.000433), $^{207}Pb/^{204}Pb$ (15.587203 ± 0.000426), $^{208}Pb/^{204}Pb$ (38.313812 ± 0.00118), $^{207}Pb/^{206}Pb$ (0.84182 ± 0.000005), $^{208}Pb/^{206}Pb$ (2.0636) $^{208}Pb/^{207}Pb$ (2.458017 ± 0.000015), $^{87}Sr/^{86}Sr$ (0.713462 ± 0.000009), and $^{143}Nd/^{144}Nd$ ($0.512229 \pm 000{,}002$) results were obtained. In addition, the value of εNd (0) was calculated using the following formula (1) ($^{\varepsilon}Nd_{(0)} = -7.98$) (the current $^{143}Nd/^{144}Nd$ value of CHUR was assumed to be 0.512638, Zhang and Wang 2001; Eker et al. 2018):

$$\varepsilon_{Nd_{(0)}}\left[\frac{\left(\frac{143Nd}{144Nd}\right)ofsample}{(143Nd/144Nd)ofCHUR}-1\right]\times 10^4 \quad (1)$$

The isotopic data of the studied samples were compared with several regions in the Alpine-Himalayan mountain belt using the $^{87}Sr/^{86}Sr$ versus $^{\varepsilon}Nd$ diagram (Fig. 2). Comparison regions are Galatia region (Early Miocene rhyolite, alkali basalt, and dacite in Central Anatolia, Wilson et al. 1997), volcanic rocks (Late Cretaceous–Paleogene trachyandesite and trachybasalt in Central Anatolia (Alpaslan et al. 2004), granitoid (Middle Anatolia, Late Cretaceous) (Köksal and Göncüoğlu 2007), Large Himalayan–Tethyan Himalayan (Paleozoic–Eocene sedimentary sequence), and Small Himalayan (Proterozoic metasedimentary) (Bracciali et al. 2015; Eker et al. 2018). The Sr–Nd isotope mixing diagram (Fig. 2) shows that the samples examined are caused by the decomposition of granitoid.

According to data evaluation of $^{207}Pb/^{206}Pb$-$^{208}Pb/^{206}Pb$ and $^{206}Pb/^{204}Pb$, and $^{207}Pb/^{206}Pb$, it was determined that the anthropogenic–soil–geogenic component properties of the soils in the study area were of geogenic origin (Figs. 3 and 4).

Agglomerative hierarchical clustering (AHC)

In this study, AHC was performed using the common correlation coefficients between the components and the components were divided into five main groups according to this analysis (Fig. 5).

Hg mineralization in the study area is located in dolomitic limestone–limestone units. Co-existence/accumulation of immobile and mobile elements can be expressed by the fact that the elements are close to the source zone and are not exposed to weathering/transporting processes too much. Therefore, it can be said that these three elements forming a group together are related to operation processes. Second group consists of Ni, V, W, Co, Cd, As, Sr, Pb, U, Sb, Ag, Au, Zn, Fe, La, Ba, Mo, and P elements. This group can be explained by the fact that the elements accumulated in the waste site after the mercury in the production was separated and the elements accumulated in the waste site act together and accumulate according to the density/mobility of the elements that came into the environment through hydrothermal processes. Third group is represented by addition of sulfur to manganese and titanium which exist in the environment. This group is thought to be caused by sulfide ore formations and hydrothermal alterations originating from granite in the region. Group 4 occurred when

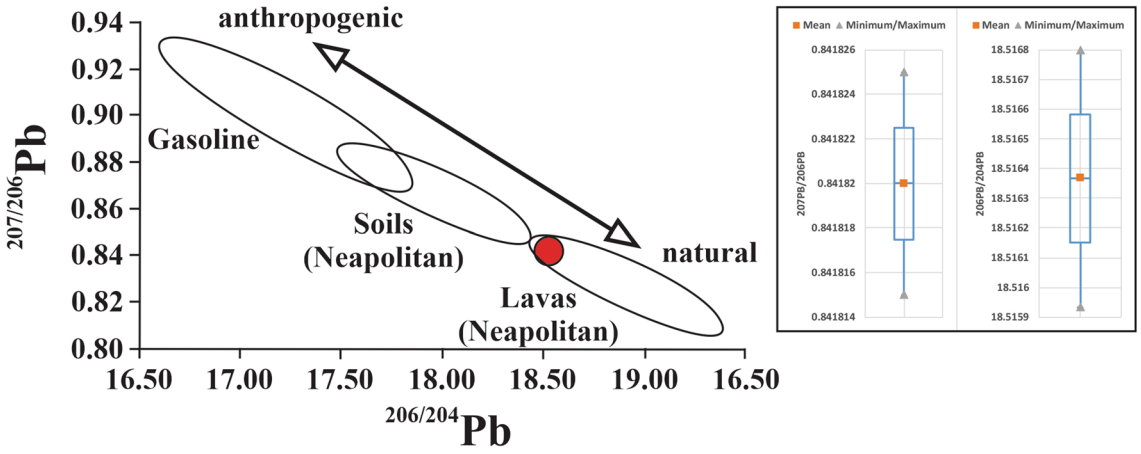

Fig. 3 Graph of $^{206}Pb/^{204}Pb$ and $^{207}Pb/^{206}Pb$ (Edited and received from Cicchella et al. 2008) and error bars on the isotope plots

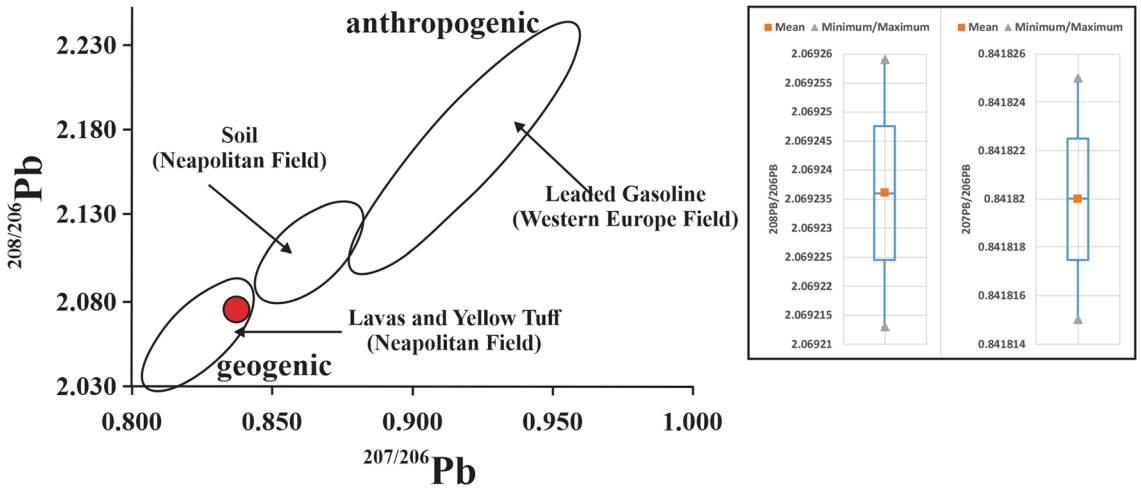

Fig. 4 Graph of $^{207}Pb/^{206}Pb$ and $^{208}Pb/^{206}Pb$ (Cicchella et al. 2008) and error bars on the isotope plots

Th and K acted together and subsequently Al was added. It is thought that the elements of this group are deposits due to the weathering of the metamorphic–granitic rocks in the region.The fifth group is represented by the addition of Cu to the group later, while Cr and Na act together. This group is associated with ophiolitic rocks (Baran and Kargı 2005) and hydrothermal alterations in the region. It is understood that there is less weathering and transportation in the environment.

Geoaccumulation index (Igeo)

In this study, depending on the concentration of As and Hg in the soil, according to the accumulation index and the evaluation of the pollution potential of the region, As_{Igeo} and Hg_{Igeo} are more prominent than Zn, Pb, Mn, Ni, Fe, Cd, As, Al, Cr, and Hg. As_{Igeo} was found extremely in S_{tez}-1, S_{tez}-2, S_{tez}-3, S_{tez}-4, S_{tez}-5, S_{tez}-6, S_{tez}-7, S_{tez}-8, S_{tez}-9, S_{tez}-10 locations, moderately at S_{tez}-18 location, unpolluted-to-moderately at S_{tez}-11, S_{tez}-12, S_{tez}-13, S_{tez}-15, S_{tez}-16, S_{tez}-17, S_{tez}-19, S_{tez}-20, and S_{tez}-21 locations, and unpolluted at S_{tez}-14 and S_{tez}-16 locations. Hg_{Igeo} was found extremely at S_{tez}-1, S_{tez}-2, S_{tez}-3, S_{tez}-4, S_{tez}-5, S_{tez}-6, S_{tez}-7, S_{tez}-8, S_{tez}-9, S_{tez}-10, S_{tez}-11, S_{tez}-19 locations, strongly to extremely at S_{tez}-20 location, strongly in S_{tez}-14 and S_{tez}-17 locations, moderately in location S_{tez}-12, and moderately-to-strongly at location S_{tez}-18 (Table 6).

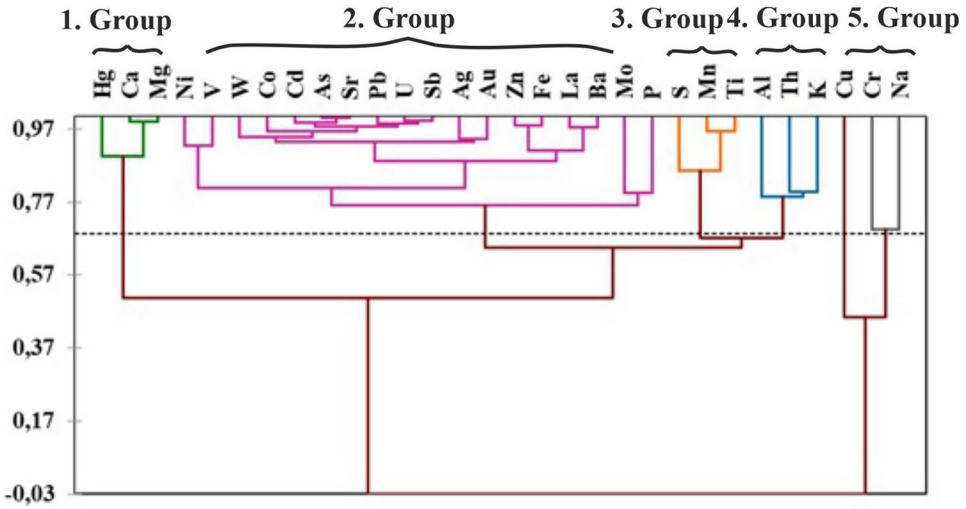

Fig. 5 Agglomerative hierarchical clustering dendrogram

Contamination factor (CF)

According to the Contamination factor of the region, depending on the concentration values of As and Hg, CF_{As} and CF_{Hg} values stand out with a significant difference. CF_{As} in S_{tez}-1, S_{tez}-2, S_{tez}-3, S_{tez}-4, S_{tez}-5, S_{tez}-6, S_{tez}-7, S_{tez}-8, S_{tez}-9, and S_{tez}-10 locations were found to be very high, S_{tez}-11, S_{tez}-12, S_{tez}-13, S_{tez}-14, S_{tez}-15, S_{tez}-16, S_{tez}-17, S_{tez}-19, S_{tez}-20, and S_{tez}-21 locations were found to be moderate, and S_{tez}-18 location was found to be considerable. CF_{Hg} was found to be very high at S_{tez}-1, S_{tez}-2, S_{tez}-3, S_{tez}-4, S_{tez}-5, S_{tez}-6, S_{te}z-7, S_{tez}-8, S_{tez}-9, S_{tez}-10, S_{tez}-11, S_{tez}-14, S_{tez}-16, S_{tez}-17, S_{tez}-18, S_{tez}-19, and S_{tez}-20 locations, considerable at S_{tez}-12 location, and moderate at S_{tez}-13, S_{tez}-15, and S_{tez}-21 locations (Table 6).

Enrichment factor (EF)

Mercury and arsenic concentration are prominent in Enrichment factor (EF) as in other factors. EF_{As}, S1, S2, S3, S4, S5, S6, S7, S8, S9, and 10 were extremely high, S11, S12, S13, S15, S16, S17, S18, S19, S20, and S21 were moderate, and S14 was found as depletion to mineral. EF_{Hg}, S1, S2, S3, S4, S5, S6, S7, S8, S9, S10, S11, S19, and S20 were found to be extremely high; S12, S13, S14, S16, S17, and S18 were found as significant; S15 and S21 moderate (Table 6). The points determined as extremely high/significant in the study area are close to the areas where the mining and operation processes take place, and the points determined as Moderate are the areas farther from the areas where the mining and operation processes take place, compared to the erosion/transportation processes depending on the morphological and gravity conditions. The area determined as depletion to mineral is located further away from the operation process in geogenic and anthropogenic terms.

Potential ecological risk factor (E_r^i)

Potential ecological risk factor (E_r^i) As and Hg stand out significantly from other elements. As was found very high at S_{tez}-1, S_{tez}-2, S_{tez}-3, S_{tez}-4, S_{tez}-5, S_{tez}-6, S_{tez}-7, S_{tez}-8, S_{tez}-9, and S_{tez}-10 locations; Hg was found very high at S_{tez}-1, S_{tez}-2, S_{tez}-3, S_{tez}-4, S_{tez}-5, S_{tez}-6, S_{tez}-7, S_{tez}-8, S_{tez}-9, S_{tez}-10, S_{tez}-11, S_{tez}-14, S_{tez}-17, S_{tez}-18, S_{tez}-19, and S_{tez}-20 locations, high at S_{tez}-12 and S_{tez}-16 locations, and considerable at S_{tez}-13, S_{tez}-15 and S_{tez}-21 locations.

Potential ecological risk index (RI)

The potential ecological risk (RI) calculation in the region has been made. According to this calculation, when the potential ecological risk index is evaluated, As and Hg are calculated as very high.

The pollution load index (PLI)

PLI results for the region were calculated according to the formula in Table 1. According to the results, values greater than 1 are considered as polluted and values less than 1 as unpolluted. When the pollution assessment of the region was evaluated according to PLI, the locations S_{tez}-1, S_{tez}-2, S_{tez}-3, S_{tez}-4, S_{tez}-5, S_{tez}-6, S_{tez}-7, S_{tez}-8, S_{tez}-9, S_{tez}-10, S_{tez}-11, and S_{tez}-19 were found as polluted and the remaining locations were found as unpolluted (Table 6).

Table 6 Evaluation of Igeo, CF, EF, and PLI results

Background*	Value	Cu	Pb	Zn	Ni	Mn	Fe	As	Cd	Cr	Al	Hg	PLI	
		45	20	95	68	850	47,200	13	0.3	90	80,000	0.4		
S_{TEZ}-1	Igeo	− 1.6	0.0	− 0.5	− 0.3	− 0.6	− 0.5	7.8	0.2	− 2.8	− 3.9	10.7	2.6	Pollution
	CFFe	0.5	1.5	1.1	1.2	1.0	1.0	340.3	1.7	0.2	0.1	2500.0		
	EF	0.5	1.4	1.0	1.2	1.0	1.0	325.1	1.6	0.2	0.1	2388.7		
S_{TEZ}- 2	Igeo	− 1.8	0.0	− 0.5	− 0.4	− 0.6	− 0.5	7.8	− 0.1	− 2.7	− 3.9	10.7	2.5	Pollution
	CFFe	0.4	1.5	1.1	1.2	1.0	1.0	338.7	1.4	0.2	0.1	2500.0		
	EF	0.4	1.5	1.0	1.1	0.9	1.0	328.3	1.3	0.2	0.1	2423.0		
S_{TEZ}- 3	Igeo	− 1.7	0.0	− 0.6	− 0.3	− 0.6	− 0.6	7.8	0.1	− 2.8	− 4.0	10.7	2.5	Pollution
	CFFe	0.5	1.5	1.0	1.2	1.0	1.0	332.7	1.6	0.2	0.1	2500.0		
	EF	0.5	1.5	1.0	1.2	1.0	1.0	329.9	1.6	0.2	0.1	2479.0		
S_{TEZ}-4	Igeo	− 1.5	0.8	− 0.1	0.4	0.2	− 0.1	9.0	0.6	− 1.9	− 2.4	9.5	3.7	Pollution
	CFFe	0.5	2.5	1.4	2.0	1.7	1.4	769.2	2.3	0.4	0.3	1102.5		
	EF	0.4	1.8	1.0	1.4	1.2	1.0	538.7	1.6	0.3	0.2	772.1		
S_{TEZ}- 5	Igeo	− 1.5	0.8	− 0.1	0.5	0.1	− 0.1	9.0	0.6	− 1.9	− 2.4	9.7	3.8	Pollution
	CFFe	0.5	2.6	1.4	2.1	1.7	1.4	769.2	2.3	0.4	0.3	1282.5		
	EF	0.4	1.8	1.0	1.4	1.2	1.0	541.1	1.6	0.3	0.2	902.1		
S_{TEZ}-6	Igeo	− 1.8	0.0	− 0.5	− 0.4	− 0.5	− 0.5	7.8	0.0	− 2.6	− 3.9	10.7	2.5	Pollution
	CFFe	0.4	1.5	1.0	1.2	1.1	1.0	334.0	1.5	0.2	0.1	2500.0		
	EF	0.4	1.5	1.0	1.1	1.0	1.0	321.8	1.4	0.2	0.1	2408.2		
S_{TEZ}-7	Igeo	− 1.8	0.1	− 0.5	− 0.4	− 0.7	− 0.5	7.8	− 0.2	− 2.7	− 4.0	10.7	2.5	Pollution
	CFFe	0.4	1.6	1.0	1.1	0.9	1.1	334.1	1.3	0.2	0.1	2500.0		
	EF	0.4	1.5	1.0	1.1	0.9	1.0	314.1	1.2	0.2	0.1	2350.6		
S_{TEZ}-8	Igeo	− 1.1	0.8	0.3	0.3	− 0.5	0.5	9.0	1.0	− 1.4	− 2.7	10.7	4.4	Pollution
	CFFe	0.7	2.6	1.9	1.9	1.0	2.1	769.2	2.9	0.6	0.2	2500.0		
	EF	0.3	1.2	0.9	0.9	0.5	1.0	366.7	1.4	0.3	0.1	1191.9		
S_{TEZ}-9	Igeo	− 1.0	1.0	0.3	0.3	− 0.5	0.5	9.0	0.8	− 1.4	− 2.6	10.7	4.4	Pollution
	CFFe	0.8	2.9	1.9	1.9	1.0	2.1	769.2	2.6	0.6	0.2	2500.0		
	EF	0.4	1.4	0.9	0.9	0.5	1.0	370.9	1.3	0.3	0.1	1205.3		
S_{TEZ}-10	Igeo	− 1.7	0.8	0.2	0.4	0.4	0.1	9.0	0.8	− 1.7	− 2.2	9.3	3.9	Pollution
	CFFe	0.5	2.6	1.7	2.0	1.9	1.6	769.2	2.6	0.5	0.3	940.0		
	EF	0.3	1.6	1.0	1.2	1.2	1.0	467.9	1.6	0.3	0.2	571.8		
S_{TEZ}-11	Igeo	− 0.6	− 0.4	− 0.5	− 0.3	− 0.7	− 0.8	0.6	− 2.0	− 1.1	− 2.9	5.1	1.2	Pollution
	CFFe	1.0	1.1	1.1	1.2	0.9	0.8	2.3	0.4	0.7	0.2	52.5		
	EF	1.2	1.4	1.3	1.5	1.1	1.0	2.8	0.4	0.8	0.2	62.9		
S_{TEZ}-12	Igeo	− 0.7	− 0.3	− 0.7	− 0.3	− 0.7	− 0.9	0.6	− 2.0	− 1.0	− 2.7	1.7	1.0	Unpollution
	CFFe	1.0	1.2	1.0	1.2	0.9	0.8	2.3	0.4	0.8	0.2	5.0		
	EF	1.2	1.4	1.1	1.5	1.1	1.0	2.8	0.4	0.9	0.3	6.0		
S_{TEZ}-13	Igeo	− 0.8	− 0.7	− 0.8	− 0.4	− 1.2	− 1.7	0.4	− 1.9	− 1.6	− 3.0	0.7	0.8	Unpollution
	CFFe	0.9	0.9	0.9	1.2	0.7	0.5	1.9	0.4	0.5	0.2	2.5		
	EF	1.8	2.0	1.8	2.4	1.4	1.0	4.1	0.8	1.1	0.4	5.2		
S_{TEZ}-14	Igeo	− 0.8	− 0.7	− 0.7	− 0.1	− 0.9	− 0.9	− 0.2	− 1.8	− 1.7	− 3.3	3.1	0.9	Unpollution
	CFFe	0.9	0.9	0.9	1.4	0.8	0.8	1.3	0.4	0.4	0.2	12.5		
	EF	1.1	1.1	1.1	1.8	1.0	1.0	1.6	0.5	0.6	0.2	15.7		
S_{TEZ}-15	Igeo	− 0.6	− 1.0	− 0.6	− 0.4	− 1.4	− 0.9	0.9	− 2.3	− 1.9	− 3.6	0.7	0.7	Unpollution
	CFFe	1.0	0.8	1.0	1.2	0.6	0.8	2.7	0.3	0.4	0.1	2.5		
	EF	1.3	1.0	1.3	1.5	0.7	1.0	3.5	0.4	0.5	0.2	3.2		
S_{TEZ}-16	Igeo	− 1.6	− 0.6	− 0.8	− 0.1	− 0.7	− 1.3	− 0.1	− 2.5	− 2.6	− 3.9	2.3	0.7	Unpollution
	CFFe	0.5	1.0	0.9	1.4	0.9	0.6	1.4	0.3	0.2	0.1	7.5		
	EF	0.8	1.5	1.4	2.3	1.5	1.0	2.3	0.4	0.4	0.2	12.0		

Table 6 (continued)

Background*	Value	Cu	Pb	Zn	Ni	Mn	Fe	As	Cd	Cr	Al	Hg	PLI	
		45	20	95	68	850	47,200	13	0.3	90	80,000	0.4		
S_{TEZ}-17	Igeo	− 0.3	− 0.3	− 1.0	− 0.2	− 1.6	− 1.5	0.6	− 2.0	− 1.9	− 4.1	3.9	0.9	Unpollution
	CFFe	1.2	1.2	0.7	1.3	0.5	0.5	2.3	0.4	0.4	0.1	22.5		
	EF	0.8	1.5	1.4	2.3	1.5	1.0	2.3	0.4	0.4	0.2	12.0		
S_{TEZ}-18	Igeo	− 0.7	− 0.7	− 0.5	− 0.6	− 1.0	− 1.0	1.2	− 2.2	− 1.3	− 3.7	2.7	0.9	Unpollution
	CFFe	0.9	0.9	1.0	1.0	0.8	0.8	3.4	0.3	0.6	0.1	10.0		
	EF	1.2	1.2	1.4	1.3	1.0	1.0	4.6	0.4	0.8	0.2	13.3		
S_{TEZ}-19	Igeo	− 0.7	− 0.9	− 0.7	− 0.9	− 0.9	− 1.0	0.9	− 2.3	− 1.3	− 3.4	5.2	1.0	Pollution
	CFFe	0.9	0.8	0.9	0.8	0.8	0.8	2.7	0.3	0.6	0.1	55.0		
	EF	1.2	1.0	1.2	1.0	1.1	1.0	3.5	0.4	0.8	0.2	71.1		
S_{TEZ}-20	Igeo	− 1.4	− 1.0	− 0.9	− 0.4	− 0.9	− 1.3	0.5	− 2.5	− 1.5	− 3.3	4.8	0.9	Unpollution
	CFFe	0.6	0.7	0.8	1.1	0.8	0.6	2.2	0.3	0.5	0.2	42.5		
	EF	0.9	1.2	1.3	1.7	1.3	1.0	3.4	0.4	0.9	0.2	67.5		
S_{TEZ}-21	Igeo	− 0.6	− 0.7	− 0.8	− 0.6	− 1.3	− 1.2	0.3	− 1.9	− 1.7	− 3.0	0.7	0.8	Unpollution
	CFFe	1.0	0.9	0.9	1.0	0.6	0.6	1.9	0.4	0.5	0.2	2.5		
	EF	1.5	1.4	1.4	1.6	1.0	1.0	2.9	0.6	0.7	0.3	3.9		

*Background value (Turekian and Wedepohl 1961)

Discussion

This study was carried out for the first time in the region with the aim of determining PTE accumulation in plants and soils, pollution risk assessment, ecological risk, impact on human health, and source and distribution in the North West region of Turkey. Mining and related activities also have a negative impact on the environment, both during mining activities and during the years after the mine is closed (Lottermoser 2007).

Soil samples can be found around the gallery (S_{tez}-1, S_{tez}-4, and S_{tez}-8) where the mercury ore is extracted, the area where the extracted ores are smelted (S_{tez}-2 and S_{tez}-3), around the landfill (S_{tez}-6, S_{tez}-7, and S_{tez}-9), and below the abandoned mine as a topographic elevation (S_{tez}-5, S_{tez}-10, S_{tez}-11, S_{tez}-19, and S_{tez}-20) and the upper part (S_{tez}-12, S_{tez}-13, S_{tez}-14, S_{tez}-15, S_{tez}-16, and S_{tez}-18). Besides, sampling was made on the ore transport route (S_{tez}-17). When the samples were taken from the point of difference from the gallery field of ecological risk and assessment the potential impact on human health, arsenic (except for S_{tez}-14 and S_{tez}-16 locations) and mercury concentration of samples taken from all locations is above the Turkey soil pollution limit values (Table 4). The accumulation of soil and plant samples around previously operated mercury mines in different countries was compared. Hg concentration in soils in Hg extracted regions such as Wanshan Hg mine and Xunyang Hg mine (China), Valle del Azogue Hg mine and, Almad en Hg mine (Spain), Hg mines, Alaska (USA) is above the values in this study (Table 7). Hg concentration is also high in soils around Hg mining sites such as Idrija Hg mine (Slovenia), Palawan Hg mine (Philippines), Yanwuping Hg mine (China), Ladik Hg mine (Turkey), Halikey Hg mine (Turkey), and Türkönü Hg mine (Turkey) (Table 7). The values in this study are significantly higher than the background value (0.0089 mg/kg) previously known in the USA (Shacklette and Boerngen, 1984). It is well above the Hg concentration value in the Turkish soil pollution regulation (Table 7) (MOEF 2001). Hg concentration in soil samples, and heavy metals such as lead, cadmium, zinc, antimony, arsenic, mercury, and strontium are often toxic pollutants that accumulate in the waste of abandoned mines (Bhattacharya et al. 2006). It is also noted that in mining sites, the number of metal pollutants can be 100–1000 times higher than the mean concentration in a given soil, and heavy-metal release increases significantly when the wastes are exposed to the atmosphere, meteoric, and surface water (Smuda et al. 2008).

Ecological pollution values come to the fore due to mercury and arsenic accumulations in Igeo, CF, EF, RI, PLI, and evaluations made according to the concentration values of PTE toxic elements at the locations where the samples were taken. According to the PLI results, S_{tez}-1, S_{tez}-2, S_{tez}-3, S_{tez}-4, S_{tez}-5, S_{tez}-6, S_{tez}-7, S_{tez}-8, S_{tez}-9, S_{tez}-10, S_{tez}-11, and S_{tez}-19 locations are polluted, where the impurities are associated with the abandoned mine operation and ore extraction, transportation, ore smelting, and mine waste, and it is thought that PTE accumulation occurs with the effect of meteoric waters and winds (Sebei et al. 2020). Besides, PTE element accumulation at the S_{tez}-17 location is on the ore transport route and is thought to occur during transport (Barkett and Akün 2018). Locations S_{tez}-12, S_{tez}-13, S_{tez}-14, S_{tez}-15,

Table 7 Comparative Hg concentrations in plant and soil at the Tezcan Hg mine to some other Hg mines worldwide

Location	Soil (ppm)	Plant (ppm)	References
Almad_en Hg mine, Spain	6–8889	2.6–298.2	Higueras et al. (2003)
Hg mines, Alaska, USA	0.03–5326	10–900	Bailey et al (2002)
Valle del Azogue Hg mine, Spain	1–2300		Navarro et al(2006)
Wanshan Hg mine, China	0.1–790		Qui et al. (2005)
Xunyang Hg mine, China	1.3–752		Zhang et al (2009)
Tezcan Hg mine, Turkey	1–500	1.3–9	This study
Palawan Hg mine, Philippines	6.9–400		Gray et al (2003)
Idrija Hg mine, Slovenia	8.9–369		Kocman et al (2004)
Yanwuping Hg mine, China	0.24–240		Qui et al. (2013)
Türkönü Hg mine, Turkey	12–42		Gemici and Tarcan (2007)
Halıköy Hg mine, Turkey	0.1–33		Gemici et al. (2009)
Ladik Hg mine, Turkey	0.2–17.6		Horasan (2020)

S_{tez}-16, and S_{tez}-18 are in the opposite direction of the slope to the location of the abandoned mine, and the origin of the PTE element accumulation here is thought to be geogenic. When the samples collected from the region were examined in terms of As (I_{geo}, CF, EF, and RI) and Hg (I_{geo}, CF, EF, and RI) values, it was observed that the origin of the accumulations in locations S_{tez}-12, S_{tez}-13, S_{tez}-14, S_{tez}-15, S_{tez}-16, and S_{tez}-18 was geogenic. The geogenic elements here are thought to be caused by the hydrothermal phase mineralizations and alterations associated with the granite intrusions in the region. The units in other locations are formations of anthropogenic origin that developed due to the activities in the abandoned mining operation. These accumulations were moved, dispersed, and accumulated downstream from the

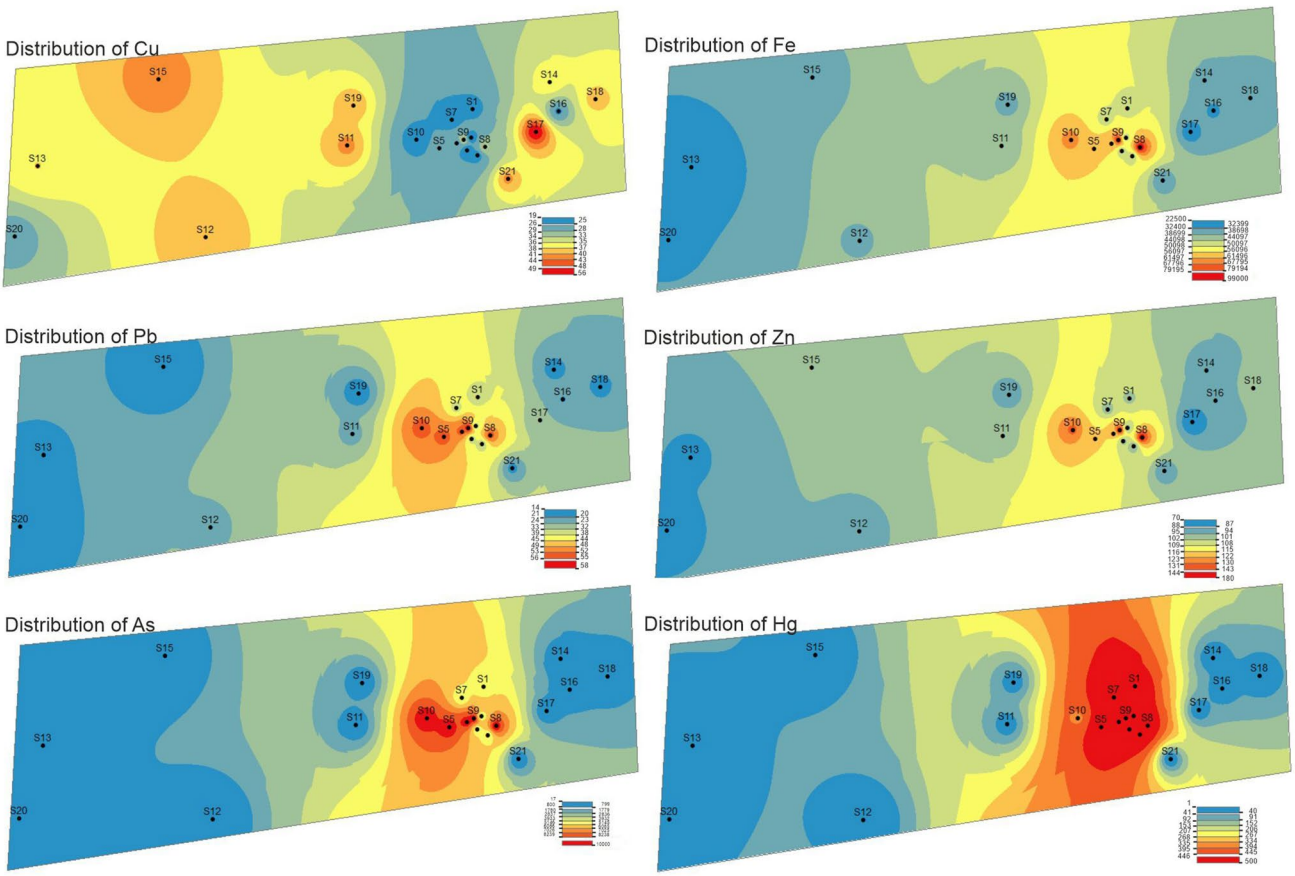

Fig. 6 Distribution of Cu, Fe, Pb, Zn, As, and Hg concentrations in the study area

point where the source (abandoned mine, smelter, and mine-waste areas) was located (Fig. 6). In the vicinity of the mineral ores, mechanical distribution of arsenic around mineral ores, and high contamination by secondary mineral products by water and air effects significantly increase the arsenic content of the soil (Garcia-Sanchez and Alverez-Ayuso 2003).

Plant species [*Mentha longifolia* subsp. *typhoides* (dere nanesi) from the Lamiaceae (Turkish name: Ballıbabagiller) family, *Taraxacum buttleri* (karahindiba) from the Asteraceae (Turkish name: Papatyagiller) family, *Plantago lanceolata* (damarlıca) from Plantaginaceae (Turkish name: Sinirotugiller) family, and *Pyracantha coccinea* (ateşdikeni) from the Rosaceae (Turkish name: Gülgiller) family (Davis 1972, 1975, 1982; Güner et al. 2012)] gathered from locations where mercury and arsenic concentrations exceed turkey soil contamination limit values were evaluated. The accumulation of toxic metals in the soil is of concern due to its negative effects on soil ecosystems and also potential health risks. The convey of trace metals from the soil to the plant is one of the main routes of human exposure to toxic metal contamination. Estimation of metal bioavailability and bioavailability in the soil is essential for the evaluation of health risks and environmental quality (Ridošková et al. 2017). Monitoring the state of environmental pollution with living organisms is one of the most important activities of environmental chemistry and is often referred to as bio-monitoring. The importance of observing the pollution status of ecosystems containing heavy metals by monitoring their contents in living organisms has been at the center of scientific studies for many years (Gosar 2008). Plant species taken from inside the plant, near the smelting plant, and from the soils near the closed plant are compatible with the PTE concentrations in the soils they are collected. There is a close relationship between metal contents in plants and metal contents in mineralized areas. Even research with soil has shown that in many cases, plants show mineralization better than soil (Gosar 2008). Samples from locations V1 (Lamiaceae family, *Mentha longifolia* subsp. *typhoides*), V4 (Asteraceae family, *Taraxacum buttleri*), and V8 (Asteraceae family, *Taraxacum buttleri*) were taken from plants grown in soils near the waste released as a result of mining activities. PTE accumulation in plants in this location is thought to develop due to wastes. The plants in V2 (Asteraceae family, *Taraxacum buttleri*) and V3 (Asteraceae family, *Taraxacum buttleri*), the soils where it grows, are close to the area where the ore is smelted, and the source of PTE accumulation in the plant here is thought to be related to melting. V6 (Plantaginaceae family, *Plantago lanceolata*), V7 (Rosaceae family, *Pyracantha coccinea*), and V9 (Plantaginaceae family, *Plantago lanceolata*) are samples taken from plants near the gallery, and the deposits in these plants are thought to have occurred during ore extraction and transport. V5 (Lamiaceae family, *Mentha longifolia* subsp. *typhoides*), V10 (Plantaginaceae family, *Plantago lanceolata*), and V11 (Plantaginaceae family, *Plantago lanceolata*) points are below the operation area as topographic elevation and are in the direction of the topographic slope. Plants take in heavy metals from the soil and their leaves are exposed to polluted air (Zurera et al. 1989). For this reason, it is thought that the PTE accumulations in the plants here were conveyed to the soils in these locations as a result of the mining and smelting processes in the operation site and accumulated in the structures of the plants. Changes in chemical types, and conversions between organic and inorganic forms can occur by changing valence during the transport process. Bioaccumulation and bioamplification potential of heavy metals are the factors that can increase the persistence of pollutants that pose a long-term risk in nature (Yang et al. 2016; Madeet al. 2016; Radulescu et al. 2014). Heavy metals are of great interest as environmental pollutants due to their ability to enter the food chain and bioaccumulation from contaminated soil (Olayinka et al. 2011). Consistent with the high Hg and As concentrations found in the soils, it was determined that the As and Hg values in the plant species in these soils locations show high-concentration values. Plants are exposed to many natural and anthropogenic factors in ecology. These must adapt to high concentrations of heavy metals that alter their metabolic processes (Seregin and Ivanov 2001; Repkina et al. 2013). It is well known that the occurrence, as well as the relative abundance of native perennials, is related to their physiological and ecological tolerance. It provides important information about the degree of environmental pollution and also has obvious effects on human health. These native plants (considered by experts to be in the weeds category) are known to be widely used for ecological restoration in soil phytoremediation processes, especially in agriculture and traditional medicine. Rural populations of many countries consider perennial plants as an alternative to the treatment of different ailments due to their psychological properties. However, people can use these plants without knowing their potential risks due to a lack of knowledge about their metal-deposition potential (Adriano 2001; Buruleanu et al. 2018; Pehoiu et al. 2020; Ozturk and Arici 2021; Coskun et al. 2021). Mercury, a global pollutant known for its long distance transport, can come from a variety of sources (geogenic and anthropogenic). Inorganic mercury, which can be absorbed negligibly in contact with the skin, can be absorbed at different rates in the lung and gastroistinal system. On the other hand, while 60–80% of elemental mercury is absorbed, it can be absorbed negligibly in the skin and gastrointestinal system (Gochfeld 2003; Zhidong et al. 2020). Besides, Hg exposure can cause kidney damage (Chanchan et al. 2020). Individuals can inadvertently ingest soil (or dust) particles by mouth by doing hand-to-mouth activities outdoors. Oral ingestion of soil or dust particles with high Hg concentrations

may pose significant exposure risks to humans, particularly children (Jimenez-Oyola et al. 2020; Zhidong et al. 2020). During the distillation process of arsenic and cinnabar ores, which are prominent in the abandoned mercury quarry and its surroundings, arsenic pollution has also occurred in the environment (Bhattacharya et al. 2006; Garcia-Ordiales et al. 2018). Poisonous As and its chemical compounds, which are dangerous carcinogenic substances, may enter the human body through skin absorption, respiration, and oral route in the natural environment (Liu et al. 2007). Long-term exposure to arsenic may increase the risk of prostate cancer, nervous system dysfunction, cardiovascular disease, and diabetes (Cantor and Lubin 2007; Coronado-González et al. 2007; Boamponsem et al. 2010).

In isotope (Pb, Sr, and Nd) studies carried out in the soil, it is stated that ^{87}Sr (Capo et al. 1998; Vanhaecke et al. 1999; Almeida and Vasconcelos 2001) is used in determining different rock types with geological age and geographical locations according to their characteristics. Besides, it is stated that the erosion of the rocks in the basement in the region is an important strontium source for the soil. In the original evaluation of $^{87}Sr/^{86}Sr$ isotopes, it was stated that high rates (0.710–0.716) were detected in alluvial sands derived from pre-Cambrian granitic and felsic rocks. It is also stated that the isotopic composition of strontium is different in Oceans ($^{87}Sr/^{86}Sr = 0.7092$), young volcanic (about 0.703), marine carbonates (about 0.708), and older continental crust (about 0.720). (Faure 1986; Aberg 1995). According to the studies, a high 87Sr/86Sr ratio is characteristic of granitic and therefore older rocks compared to the values determined from the study area (Costa 2006; Martins et al 2014). Besides, according to the evaluations of $^{206}Pb/^{204}Pb$ with $^{207}Pb/^{206}Pb$ and $^{207}Pb/^{206}Pb$ and $^{208}Pb/^{206}Pb$ (against), the source origin of Pb was thought to be due to the mineralizations/alterations in the region and its immediate surroundings.

In the AHC formed according to the data obtained, the elements were divided into 5 main groups, taking into account the ability of the elements/minerals to act together in the operation area, gallery area, waste area, and geological processes. The first, second, third, and fourth groups of these groups represent the movement of elements that occur as a result of anthropogenic events, and the fifth group is represented by the movement of elements that are separated as a result of geogenic events.

In this study, the effects of PTE accumulation on the soil and plants around the abandoned mercury quarry on the environment and humans were investigated. In the case of PTE mixing with ground and surface waters, the investigation of its removal, its distribution (Bhatti et al.2020; Buaisha et al.2020), and its effects on human health (Yildiz et al.2008; Nalbantcilar and Pinarkara 2016; Cetin et al.2017), a study on the effect of the river passing through the study area and the groundwater in the vicinity will be complementary using the data obtained from this study.

Conclusions

There have been many publications about the environmental impact of abandoned mercury quarries in recent years (Gray et al. 2015; Kulikova et al. 2019; Hadjipanagiotou et al. 2020; Horasan 2020). In this study, it was determined that the accumulation of mercury and arsenic in the soils in the samples taken from the soil and plants around the abandoned mine, smelter, and waste site was significantly higher than the limit values of soil pollution in Turkey.

When compared with 11 Hg mines in some countries in the world, Idrija Hg mine (Slovenia), Palawan Hg mine (Philippines), Yanwuping Hg mine (China), Türkönü Hg mine, Halıköy Hg mine, and Ladik Hg mine (Turkey) Hg concentration was found to be higher than the Hg concentration compared to the studies conducted on plants around Alaska (USA) and Almad en Hg enamel (Spain).

In the abandoned Tezcan Hg mining field, the distribution down the slope has occurred from the area where the mining activities are the source of the distribution of Hg and As. The relationship with the granite intrusions in the region at codes higher than the altitude of the mining activity or in areas above the slope limited by topographic barriers is due to the accumulation of ore rocks undergoing hydrothermal phase mineralization and alteration.

The concentration of mercury and arsenic in plants reflects the high-concentration values in the soil. It is thought that while arsenic–mercury concentrations in the soil and plant structure near the operation site are above the limit values, the concentration values decrease in locations far from the source and the accumulation in the locations is geogenic. The high amount of arsenic and mercury accumulation in the region has high ecological risk factors for living life and it is thought that it may cause serious problems in terms of human health if it is included in the food chain. For this reason, it is considered appropriate to carry out improvement studies in the abandoned mine and surrounding areas where PTE accumulation is intense.

Author contributions Concept planning of this study was carried out by BYH. Field studies (geological, soil and plant), sampling (soil and plant), evaluation of results, mapping, and statistical studies conducted in the study area were carried out by AO and BYH. Naming, description, and properties of plants were carried out by OT. All authors have read and approved this article.

Availability of data and materials The datasets used and/or analyzed during the current study are available from the corresponding author on reasonable request. All data generated or analyzed during this study are included in this published article.

Declarations

Conflict of interest The authors declare that they have no competing interests.

References

Aberg G (1995) The use of natural strontium isotopes as tracers in environmental studies. Water Air Soil Pollut 79(1–4):309–322. https://doi.org/10.1007/bf01100444

Adriano DC (2001) Trace elements in terrestrial environments biogeochemistry, bioavailability and risk of metals, 2nd edn. Springer-Verlag, New York

Almeida CM, Vasconcelos MTSD (2001) ICP-MS determination of strontium isotope ratio in wine in order to be used as a fingerprint of its regional origin. J Anal at Spectrom 16:607–611

Alpaslan M, Frei R, Boztug D, Kurt MA, Temel A (2004) Geochemical and Pb-Sr-Nd isotopic constraints indicating an enriched-mantle source for late cretaceous to early tertiary volcanism, central Anatolia. Int Geol Rev 46:1022–1041

Altay T, Duplıpinar İ (2013) Geologic and mineralogic ınvestigations on clays from coal deposits in Dinar (Afyon)-Baklan (Denizli) region, western Turkey. AKU J Sci Eng. https://doi.org/10.5578/fmbd.6425

Alvarez A, Saez JM, Costa JSD, Colin VL, Fuentes MS, Cuozzo SA, Benimeli CS, Polti MA, Amoroso MJ (2017) Actinobacteria: current research and perspectives for bioremediation of pesticides and heavy metals. Chemosphere 166:41–62. https://doi.org/10.1016/j.chemosphere.2016.09.070

Bailey EA, Gray JE, Theodorakos PM (2002) Mercury in vegetation and soils at abandoned mercury mines in southwestern Alaska, USA. Geochem Explor Environ Anal 2(3):275–285

Baran HA, Kargı H (2005) The origin of chromites and basic dikes around andızlık—Zımparalık (Muğla). J Fac Eng Arch Selcuk Univ 20(4):65–76

Barkett MO, Akün E (2018) Heavy metal contents of contaminated soils and ecological risk assessment in abandoned copper mine harbor in Yedidalga. Northern Cyprus Environ Earth Sci 77:378. https://doi.org/10.1007/s12665-018-7556-6

Beane SJ, Comber SDW, Rieuwerts J, Long P (2016) Abandoned metal mines and their impact on receiving waters: a case study from Southwest England. Chemosphere 153:294–306. https://doi.org/10.1016/j.chemosphere.2016.03.022

Bhattacharya A, Routh J, Jacks G, Bhattacharya P, Mörth M (2006) Environmental assessment of abandoned mine tailings in Adak, Västerbotten district (northern Sweden). Appl Geochem 21(10):1760–1780

Bhatti ZA, Qureshi K, Maitlo Ahmed S (2020) Study of PAN fiber and iron ore adsorbents for arsenic removal. Civ Eng J 6(3):548–562. https://doi.org/10.28991/cej-2020-03091491

Boamponsem LK, Ada JI, Dampare SB, Nyarko BJB, Essumang DK (2010) Assessment of atmospheric heavy-metal deposition in the Tarkwa gold mining area of Ghana using epiphytic lichens. Nucl Instrum Methods Phys Res Sect B 268(9):1492–1501

Bracciali L, Najman Y, Parrish RR, Akhter SH, Millar I (2015) The Brahmaputra tale of tectonic and erosion: early miocene river capture in the Eastern Himalaya. Earth Planet Sci Lett 415:25–37

Buaisha M, Balku S, Yaman SO (2020) Heavy metal removal investigation in conventional activated sludge systems. Civ Eng J 6(3):470–477. https://doi.org/10.28991/cej-2020-03091484

Buruleanu LC, Radulescu C, Georgescu AA, Danet FA, Olteanu RL, Nicolescu CM, Dulama ID (2018) Statistical characterization of the phytochemical characteristics of edible mushroom extracts. Anal Lett 51:1039–1059

Cantor KP, Lubin JH (2007) Arsenic, internal cancers, and issues in inference from studies of low-level exposures in human populations. Toxicol Appl Pharmacol 222(3):252–257

Capo RC, Stewart BW, Chadwick OA (1998) Strontium isotopes as tracers of ecosystem processes : theory and methods. Geoderma 82:197–225

Cetin I, Nalbantcilar MT, Tosun K et al (2017) How trace element levels of public drinking water affect body composition in Turkey. Biol Trace Elem Res 175:263–270. https://doi.org/10.1007/s12011-016-0779-z

Chanchan Z, Chunfang G, Li D, Min X, Aihua Z, Ping L (2020) Maternal inorganic mercury exposure and renal effects in the Wanshan mercury mining area, southwest China. Ecotoxicol Environ Saf 189:109987. https://doi.org/10.1016/j.ecoenv.2019.109987

Chen Y, Jiang Y, Huang H, Mou L, Ru J, Zhao J, Xiao S (2018) Long-term and high-concentration heavy-metal contamination strongly influences the microbiome and functional genes in Yellow River sediments. Sci Total Environ 637–638:1400–1412. https://doi.org/10.1016/j.scitotenv.2018.05.109

Chow TJ, Johnstone MS (1965) Lead isotopes in gasoline and aerosols of Los Angeles Basin, California. Science 147:502–503

Cicchella D, De Vivo B, Lima A, Albanese S, McGill RAR, Parrish RR (2008) Heavy metal pollution and Pb isotopes in urban soils of Napoli, Italy. Geochem Explor Environ Anal 8(1):103–112. https://doi.org/10.1144/1467-7873/07-148

Coronado-Gonzalez JA, Del Razo LM, Garcia-Vargas G, Sanmiguel-Salaza F, Escobedode LPJ (2007) Inorganic arsenic exposure and type 2 diabetes mellitus in Mexico. Environ Res 104(3):383–389

Coskun A, Horasan BY, Ozturk A (2021) Heavy metal distribution in stream sediments and potential ecological risk assessment in Konya Northeast region. Environ Earth Sci 80:181. https://doi.org/10.1007/s12665-021-09495-9

Costa MMCP (2006) Geoquímica de Granitóides de Pera Velha-Vila Nova de Paiva-Ferreira de Aves. M.Sc.Thesis, Universidade de Aveiro, Portugal

Coteli E, Karatas F (2017) Investigation of amounts of vitamins a, e, c, β-carotene, lycopene, glutathione and malondialdehyde in red fruit pyracantha coccinea roemer var. Lalandi. Fırat Univ J Sci 29(1):41–46

Cuvier A, Pourcelot L, Probst A, Prunier J, Roux GL (2016) Trace elements and Pb isotopes in soils and sediments impacted by uranium mining. Sci Total Environ 566–567:238–249

Davis PH (1972) Flora of Turkey and the east aegean islands v: 4. Edinburgh Universty Press, Edinburgh

Davis PH (1975) Flora of Turkey and the east aegean islands v: 5. Edinburgh Universty Press, Edinburgh

Davis PH (1982) Flora of Turkey and the east aegean islands v: 7. Edinburgh Universty Press, Edinburgh

Dengiz O, Saygın F, Imamoglu A (2016) Determination of physiographic factors, different soil classes based on st/wrb and mapping in İnebolu watershed. In: International geography symposium, 13–14 Oct 2016, Ankara

Durguti V, Aliu S, Laha F, Feka F (2020) Determination of iron, copper and zinc in the wine by FAAS. Emerg Sci J 4(5):411–417. https://doi.org/10.28991/esj-2020-01240

Eker ÇS, Sipahi F, Gümüş MK, Özkan Ö (2018) Tracing provenance and chemical weathering changes in Ankara Stream sediments, central Turkey: geochemical and Sr–Nd–Pb–O isotopic evidence. J Afr Earth Sci 138:367–382. https://doi.org/10.1016/j.jafrearsci.2017.11.034

Faure G (1986) Principles of isotope geology, 2nd edn. Wiley, New York

Garcia-Ordiales E, Covelli S, Rico JM, Roqueñí N, Fontolan G, Flor-Blanco G, Cienfuegos P, Loredo J (2018) Occurrence and speciation of arsenic and mercury in estuarine sediments affected by mining activities (Asturias, northern Spain). Chemosphere 198:281–289. https://doi.org/10.1016/j.chemosphere.2018.01.146

Garcia-Sanchez A, Alverez-Ayuso E (2003) Arsenic in soils and waters and its relation to geology and mining activities (Salamanca province, Spain). J Geochem Explor 80:69–79

Gemici U, Tarcan G (2007) Assessment of the pollutants in farming soils and waters around untreated abandoned turkonu mercury mine (Turkey). Bull Environ Contam Tox 79:20–24. https://doi.org/10.1007/s00128-007-9087-9

Gemici U, Tarcan G, Somay AM, Akar T (2009) Factors controlling the element distribution in farming soils and water around the abandoned Halıköy mercury mine (Beydağ, Turkey). Appl Geochem 24(10):1908–1917. https://doi.org/10.1016/j.apgeochem.2009.07.004

Gochfeld M (2003) Cases of mercury exposure, bioavailability, and absorption. Ecotoxicol Environ Saf 56:174–179. https://doi.org/10.1016/S0147-6513(03)00060-5

Gosar M (2008) Mercury in river sediments, floodplains and plants growing thereon in drainage area of Idrija mine, Slovenia. Polish J of Environ Stud 17(2):227–236

Gray JE, Greaves IA, Bustos DM, Krabbenhoft DP (2003) Mercury and methylmercury contents in mine-waste calcine, water, and sediment collected from the Palawan Quicksilver Mine. Philippines Environ Geol 43(3):298–307. https://doi.org/10.1007/s00254-002-0626-8

Gray JE, Theodorakos PM, Fey DL, Krabbenhoft DP (2015) Mercury concentrations and distribution in soil, water, mine waste leachates, and air in and around mercury mines in the Big Bend region, Texas, USA. Environ Geochem Health 37(1):35–48. https://doi.org/10.1007/s10653-014-9628-1

Gulson BL, Mizon KJ, Davis JD, Palmer JM, Vimpani G (2004) Identification of sources of lead in children in a primary Zn–Pb smelter environment. Environ Health Perspect 112:52–60

Güner A, Aslan S, Ekim T, Vural M, Babaç MT (2012) Türkiye Bitkileri Listesi (Damarlı Bitkiler). Nezahat Gökyiğit Botanik Bahçesi ve Flora Araştırma Derneği Yayını. İstanbul

Hakanson L (1980) An ecological risk index for aquatic pollution control. A sedimentological approach. Water Res 8:975–1001. https://doi.org/10.1016/0043-1354(80)90143-8

Hadjipanagiotou C, Christou A, Zissimos AM et al (2020) Contamination of stream waters, sediments, and agricultural soil in the surroundings of an abandoned copper mine by potentially toxic elements and associated environmental and potential human health–derived risks: a case study from Agrokipia, Cyprus. Environ Sci Pollut Res 27:41279–41298. https://doi.org/10.1007/s11356-020-10098-3

Higueras P, Oyarzun R, Biester H, Lillo J, Lorenzo S (2003) A first insight into mercury distribution and speciation in soils from the Almad_en mining district, Spain. J Geochem Explor 80(1):95e104. https://doi.org/10.1016/S0375-6742(03)00185-7

Horasan BY (2020) The environmental impact of the abandoned mercury mines on the settlement and agricultural lands; Ladik (Konya, Turkey). Environ Earth Sci 79:1–13. https://doi.org/10.1007/s12665-020-08985-6

Horasan BY, Arık F (2019) Assessing heavy metal pollution in the surface soils of central anatolia region of Turkey. Carpathian J Earth Environ Sci 14:107–118. https://doi.org/10.26471/cjees/2019/014/063

Horvat M (2002) Mercury as a global pollutant. Anal Bioanal Chem 374:981–982. https://doi.org/10.1007/s00216-002-1605-3

Jimenez-Oyola S, Garía-Martínez M, Ortega MF, Bolonio D, Rodríguez Esbrí J, Llamas JF, Higuera P (2020) Multi-pathway human exposure risk assessment using Bayesian modeling at the historically largest mercury mining district. Ecotoxicol Environ Saf 201:110833. https://doi.org/10.1016/ecoenv.2020.110833

Kabata-Pendias A (2004) Soil–plant transfer of trace elements—an environmental issue. Geoderma 122(2–4):143–149. https://doi.org/10.1016/j.geoderma.2004.01.004

Kara K, Guclu BK, Aktug E, Baytok E (2015) The determination of nutrient matter composition and in vitro digestion parameters of narrow-leaf plantain (plantago lanceolata) in ruminant. J Health Sci 24:149–155

Karatas H (2007) The ethnobotanical features of Ilgaz (Çankırı) District. Dissertation, Gazi University Institute of Science and Technology

Kocman D, Horvat M, Kotnik J (2004) Mercury fractionation in contaminated soils from the Idrija mercury mine region. J Environ Monit 6(8):696–703

Köksal S, Göncüoğlu C (2007) Sr and Nd isotopic characteristics of some S-, I- and a-type granitoids from central Anatolia. Turk J Earth Sci 17:111–127

Kong HM, Teng YG, Song LT, Wang JS, Zhang L (2018) Lead and strontium isotopes as tracers to investigate the potential sources of lead in soil and groundwater: a case study of the Hun River alluvial fan. Appl Geochem 97:291–300

Kulikova T, Hiller E, Jurkovič Ľ et al (2019) Total mercury, chromium, nickel and other trace chemical element contents in soils at an old cinnabar mine site (Merník, Slovakia): anthropogenic versus natural sources of soil contamination. Environ Monit Assess 191:263. https://doi.org/10.1007/s10661-019-7391-6

Li X, Bond PL, Huang L (2017) Diversity of as metabolism functional genes in Pb-Zn mine tailings. Pedosphere 27:630–637. https://doi.org/10.1016/S1002-0160(17)60357-6

Liu GJ, Zheng LG, Duzgoren-Aydin NS, Gao LF, Liu JH, Pen ZC (2007) Health effects of arsenic, fluorine, and selenium from indoor burning of Chinese coal. Rev Environ Contam Toxicol 189:89–106

Lottermoser BG (2007) Mine wastes. Characterization, treatment, environmental impacts, 2nd edn. Springer, New York

Madeet M, Yin Y, Zhang D, Liu J (2016) Methods and recent advances in speciation analysis of mercury chemical species in environmental samples: a review. Chem Spec Bioavailab 28:51–65. https://doi.org/10.1080/09542299.2016.1164019

Mammola S, Cardoso P, Culver DC, Deharveng L, Ferreira RL, Fišer C, Galassi DMP, Griebler C, Halse S, HumphreysWF IM, Malard F, Martinez A, Moldovan OT, Niemiller MI, Pavlek M, Reboleira ASPS, Souza-Silva M, Teeling EC, Wynne JJ, Zagmajster M (2019) Scientists warning on the conservation of subterranean ecosystems. Bioscience 69:641–650. https://doi.org/10.1093/biosci/biz064

Martins P, Madeira M, Monteiro F, De Sousa R, Curvelo-Garcia A, Catarino S (2014) 87Sr/86Sr ratio in vineyard soils from Portuguese denominations of origin and its potential for origin authentication. J Int Sci Vigne Vin 48:21–29

Mileusnic M, Mapani BS, Kamona AF, Ruzicic S, Mapaure I, Chimwamurombe PM (2014) Assessment of agricultural soil contamination by potentially toxic metals dispersed from improperly disposed tailings, Kombat mine, Namibia. J Geochem Explor. https://doi.org/10.1016/j.gexplo.2014.01.009

MOEF (2001) Ministry of environment and forestry standards. Soil pollution and controlling regulation of Turkey. Official Newspaper, number 24609, dated 10 Dec 2001

Muller G (1969) Index of geoaccumulation in sediments of the Rhine River. Geo J 2:108–118

Nalbantcilar MT, Pinarkara SY (2016) Public health risk assessment of groundwater contamination in Batman. Turkey J Water Health 14(4):650–661. https://doi.org/10.2166/wh.2016.290

Navarro A, Biester H, Mendoza JL, Cardellach E (2006) Mercury speciation and mobilization in contaminated soils of the Valle del Azogue Hg mine (SE, Spain). Environ Geol 49:1089–1101. https://doi.org/10.1007/s00254-005-0152-6

Olayinka KO, Oyeyiola AO, Odujebe FO, Oboh B (2011) Uptake of potentially toxic metals by vegetable plants grown on contaminated soil and their potential bioavailability using sequential extraction. J Soil Sci Environ Manag 2(8):220–227

Ozturk A, Arici OK (2021) Carcinogenic-potential ecological risk assessment of soils and wheat in the eastern region of Konya (Turkey). Environ Sci Pollut Res 28:15471–15484. https://doi.org/10.1007/s11356-020-11697-w

Pehoiu G, Murarescu O, Radulescu C et al (2020) Heavy metals accumulation and translocation in native plants grown on tailing dumps and human health risk. Plant Soil 456:405–424. https://doi.org/10.1007/s11104-020-04725-8

Qiu G, Feng X, Wang S, Shang L (2005) Mercury and methylmercury in riparian soil, sediments, mine-waste calcines, and moss from abandoned Hg mines in east Guizhou province, southwestern China. Appl Geochem 20(3):627–638. https://doi.org/10.1016/j.apgeochem.2004.09.006

Qiu G, Feng X, Meng B, Zhang C, Gu C, Du B, Lin Y (2013) Environmental geochemistry of an abandoned mercury mine in Yanwuping, Guizhou Province, China. Environ Res 125:124–130

Radulescu C, Stihi C, Dulama ID (2014) Elemental analysis methods for particulate matter. Chemical speciation. Analytical method validation. In: Iordache S, Dunea D (eds) Methods for the assessment of air pollution with particulate matter to children's health. MatrixROM, Bucharest, pp 119–188

Repkina NS, Talanova VV, Titov AF (2013) Influence of heavy metals on gene expression in plants. Tr Karel Nauch Tsentra Ros Akad Nauk 3:31–45

Ridošková A, Dočekalová H, Pelcová P (2017) Prediction of cadmium, lead and mercury availability to plants: a comparison between diffusive gradients measured in a thin films technique and soil grew plants. J Elem 22(1):349–363. https://doi.org/10.5601/jelem.2016.21.2.1075

Rieuwerts JS, Austin S, Harris EA (2009) Contamination from historic metal mines and the need for non-invasive remediation techniques: a case study from Southwest England. Environ Monit Assess 148:149–158. https://doi.org/10.1007/s10661-007-0146-9

Sebei A, Chaabani A, Abdelmalek-Babbou C et al (2020) Evaluation of pollution by heavy metals of an abandoned Pb-Zn mine in northern Tunisia using sequential fractionation and geostatistical mapping. Environ Sci Pollut Res 27:43942–43957. https://doi.org/10.1007/s11356-020-10101-x

Seregin IV, Ivanov VG (2001) Physiological aspects of cadmium and lead toxic effects in higher plants. Russ J Plant Physiol 48(4):606–630

Smuda J, Dold B, Spangenberg JE, Pfeifer HR (2008) Geochemistry and stable isotope composition of fresh alkaline porphyry copper tailings: implications on sources and mobility of elements during transport and early stages of deposition. Chem Geol 256(1–2):62–76

Steinmann M, Stille P (1997) Rare earth element behavior and Pb, Sr, Nd isotope systematics in a heavy-metal contaminated soil. Appl Geochem 12(5):607–623. https://doi.org/10.1016/S0883-2927(97)00017-6

Tomlinson DL, Wilson JG, Harris CR, Jeffney DW (1980) Problems in the assessment of heavy metal levels in estuaries and the formation of pollution index Helgol Wiss. Meeresunters 33:566–572. https://doi.org/10.1007/BF02414780

Turekian KK, Wedepohl KH (1961) Distribution of the elements in some major units of the earth's crust. Bull Geol Soc Am 72(2):175–192. https://doi.org/10.1130/0016-7606(1961)72[175:DOTEIS]2.0.CO;2

Uguz MF, Sevin M (2007) Turkey geology maps sheet MTA E32 technical report no: 32, Ankara

Vanhaecke F, de Wannemacker G, Moens L, Hertogen J (1999) The determination of strontium isotope ratios by means of quadrupole-based ICP-mass spectrometry: a geochronological case study. J Anal At Spectrom 14:1691–1696

Wenbo R, Jiedong Y, Jun C, Gaojun L (2006) (2006) Sr-Nd isotope geochemistry of eolian dust of the arid-semiarid areas in China: implications for loess provenance and monsoon evolution. Chin Sci Bull 51(12):1401–1412. https://doi.org/10.1007/s11434-006-2008-1

Wilson M, Tankut A, Güleç N (1997) Tertiary volcanism of the Galatia province, north-west central Anatolia, Turkey. Lithos 42:105–121

Xiao R, Wang S, Li R, Wang JJ, Zhang Z (2017) Soil heavy metal contamination and health risks associated with artisanal gold mining in Tongguan, Shaanxi, China. Ecotoxicol Environ Saf 141:17–24. https://doi.org/10.1016/j.ecoenv.2017.03.002

Yalcin MG, Coskun B, Nyamsari DG et al (2019) Geomedical, ecological risk, and statistical assessment of hazardous elements inshore sediments of the Iskenderun Gulf, Eastern Mediterranean. Turkey Environ Earth Sci 78:438. https://doi.org/10.1007/s12665-019-8435-5

Yang Y, Li Y, Zhang J (2016) Chemical speciation of cadmium and lead and their bioavailability to cole (*Brassica campestris* L.) from multi-metals contaminated soil in Northwestern China. Chem Spec Bioavailab 28:33–41. https://doi.org/10.1080/09542299.2016.1157005

Yi Y, Yang Z, Zhang S (2011) Ecological risk assessment of heavy metals in sediment and human health risk assessment of heavy metals in fishes in the middle and lower reaches of the Yangtze River basin. Environ Pollut 159:2575–2585

Yildiz A, Karaca M, Biceroglu S, Nalbantcilar MT, Coskun U, Arik F, Turkoglu C (2008) Effect of chronic arsenic exposure from drinking waters on the QT interval and transmural dispersion of repolarization. J Int Med Res 36:471–478. https://doi.org/10.1177/147323000803600311

Zhang C, Wang L (2001) Multi-element geochemistry of sediments from the Pearl River system. China Apple Geochem 16:1251–1259

Zhang L, Jin Y, Lu J, Zhang C (2009) Concentration, distribution, and bioaccumulation of mercury in the Xunyang mercury mining area, Shaanxi Province, China. Appl Geochem 24(5):950–956. https://doi.org/10.1016/j.apgeochem.2009.02.027

Zhidong X, Qinhui L, Xiaohang X, Xinbin F, Longchao L, Lin L, Chan L, Zhuo C, Guangle Q (2020) Multi-pathway mercury health risk assessment, categorization and prioritization in an abandoned mercury mining area: a pilot study for implementation of the Minamata Convention. Chemosphere 260:127582. https://doi.org/10.1016/j.chemosphere.2020.127582

Zoller WH, Gladney ES, Duce RA (1974) Atmospheric concentrations and sources of trace metals at the south pole. Science 183(4121):198–200. https://doi.org/10.1126/science.183.4121.198

Zurera G, Moreno R, Salmeron J, Pozo R (1989) Heavy metal uptake from greenhouse border soils for edible vegetables. J Sci Food Agric 49:307–314. https://doi.org/10.1002/jsfa.2740490307